ASSESSMENT OF IN VIVO TOXICITY INDUCED BY MANGANESE DIOXIDE NANOPARTICLES (MnO_2-NPs) IN SWISS ALBINO MICE (*MUS MUSCULUS*)

A Dissertation for

Course code and Course Title: ZOO – 651: Dissertation

Credits: 16 credits

Submitted in partial fulfilment of Master's Degree

M. Sc. Zoology

by

DIALLA PERPETUAL FERNANDES

Seat Number: 22P0440009

ABC ID: 628325564717

PR. Number: 201908061

Under the Supervision of

DR. AVELYNO D'COSTA

Zoology Discipline

School of Biological Sciences and Biotechnology

Goa University

6 May 2024

Seal of the School

Examined by:

DECLARATION BY STUDENT

I hereby declare that the data presented in this Dissertation report entitled, **"Assessment of in vivo toxicity induced by Manganese Dioxide nanoparticles (MnO_2-NPs) in Swiss Albino mice (*Mus musculus*)"** is based on the results of investigations carried out by me in the Zoology Discipline at the School of Biological Sciences and Biotechnology, Goa University under the supervision of Dr. Avelyno D'Costa and the same has not been submitted elsewhere for the award of a degree or diploma by me. Further, I understand that Goa University or its authorities will not be responsible for the correctness of observations / experimental or other findings given the dissertation.

I hereby authorize the university authorities to upload this dissertation on the dissertation repository or anywhere else as the UGC regulations demand and make it available to any one as needed.

Dialla Perpetual Fernandes
Seat No: 22P0440009

Date:

Place: Goa University

COMPLETION CERTIFICATE

This is to certify that the dissertation report **"Assessment of in vivo toxicity induced by Manganese Dioxide Nanoparticles (MnO_2-NPs) in Swiss Albino mice (*Mus musculus*)"** is a bonafide work carried out by **Ms. Dialla Perpetual Fernandes** under my supervision in partial fulfilment of the requirements for the award of the degree of Masters of Science in Zoology Discipline at School of Biological Sciences and Biotechnology, Goa University.

Date:

Dr. Avelyno D'Costa
Assistant Professor
Zoology Discipline

Dr. Bernard F. Rodrigues
Dean
School of Biological Science and Biotechnology
Date: 8-4-24
Place: Goa University

Dean of School of Biological Sciences
& Biotechnology
Goa University, Goa-403206

SBSB, M.Sc., Zoology
Taleigao Plateau, Goa 403206
GOA UNIVERSITY

School Stamp

PREFACE

This thesis is submitted in fulfillment of the requirement for the degree of Masters in Zoology and comprises research work carried out by the author under the guidance of Dr. Avelyno H. D'costa Assistant Professor of Zoology, Goa University from 2022 to 2023.

Manganese Dioxide Nanoparticles (MnO2-NPs) are rapidly growing in their applicative dynamism. due to their unusual physicochemical properties. Simultaneously, their exposure to aquatic organisms, humans and the environment is also increasing either by directly via its potential uses in the field of biomedicine or indirectly through the disposal of various industrial by-products. This can adversely affect various levels of biological organization, including organs, tissues, cells, subcellular structures, and proteins within living organisms. Thus, by investigating the effects of MnO2-NPs on Mus musculus, one will gain insights about its toxicity on vital organs that can be further used to generate preventive measures to reduce MnO2-NPs exposure in humans.

There are very few studies undertaken to analyze the toxicity of MnO2-NPs via oral gavage. This thesis contributes to the knowledge of investigating the toxicity of MnO2-NPs on the anatomy and physiology of the Liver and Kidney tissues in Mus musculus

The thesis is divided into five main chapters. The first chapter deals with an introduction giving applications, properties, background, sources and general toxicity of MnO2-NPs, the gap in the study (Lacunae), Hypothesis, and objectives of the study. The 2nd chapter includes a literature review of the work. Chapter 3 gives the material and methods used for the study, Mus musculus as an animal model, the test substance, experimental setup, maintenance techniques, general examinations, histological analysis, estimation of biomolecules and enzymes, assessment of genotoxicity and Statistical Analysis.

Chapter 4 represents the results embodying observations of animal behavior, estimation of different biomolecules and enzymes, genetic and histological changes occurring in the liver and kidney tissues of Mus musculus. The last chapter, i.e. Chapter 5 gives elaborate discussions, the reasons and the effects of changes occurring in the Liver and the kidney tissues of mice under the influence of MnO2-NPs are discussed. Conclusion with a summary, future work references, and contributions from the thesis follows chapter 6. And lastly Chapter 7 include all the references cited from various research articles, journals and books.

ACKNOWLEDGMENT

With the tremendous support, direction, and assistance of many people all around me throughout the period, the most difficult, energizing, and insightful trip of this project has come to an end. I would like to express my gratitude to my guide Dr. Avelyno H. D'costa who gave me the golden opportunity to do this wonderful work thereby making me realize my potential capabilities. His guidance and immense support were an indispensable part of the dissertation tenure. I am also thankful to Professor Bernard F. Rodrigues, Dean of School of Biological Sciences and Biotechnology, for the facilities equipped to make this project smoothly feasible. I also express my gratitude to Dr. Nitin S. Sawant, Programme Director of the Zoology Programme for his keen trust in providing the laboratory, and animal house facilities to conduct the work and his encouragement to bring out the best of my ability. I'm deeply grateful to Dr. Shanti N. Dessai, Dr. Minal D. Shirodkar, Dr. Preeti Pereira and Ma'am Gandhita V. Kundaikar, Assistant professors of the Zoology Department, for their endless support and priceless suggestions offered during the entire tenure of my project.

\I would also like to express my sincere gratitude to the laboratory staff and non-teaching staff of the Zoology Discipline that is, Ma'am Hina, Sir Diptesh, Sir Madhukar and Sir Vitthal for their support, patient cooperation and for providing all the necessary types of equipment and requisite information to complete my final internship. I am affectionately thankful to my friends Sania Bapari, Priyanka satarkar, Riddhi Savoiverekar and PhD Scholar Sarita Rebello for all their help. Finally, I would also like to thank and praise the almighty Lord for good health and the many blessings he has bestowed upon me, and my parents for their constant support and motivation throughout this period.

TABLES

SR.NO	TITLE	PAGE
1	Dose concentration	23
2	Pearson's Correlation between different biomolecules and enzymes	55

FIGURES

SR. NOS	TLTLE	PAGE NOS
1	Effect of MnO_2-NPs on carbohydrate concentration	45
2	Effect of MnO_2-NPs on free sugars concentration	45
3	Effect of MnO_2-NPs on protein concentration	46
4	Effect of MnO_2-NPs on albumin concentration	46
5	Effect of MnO_2-NPs on bilirubin concentration	47
6	Effect of MnO_2-NPs on TBARS concentration	48
7	Effect of MnO_2-NPs on GSH concentration	48
8	Effect of MnO_2-NPs on catalase concentration	49
9	Effect of MnO_2-NPs on SOD concentration	49
10	Effect of MnO_2-NPs on ALT concentration	50
11	Effect of MnO_2-NPs on ALP concentration	50
12	Effect of MnO_2-NPs on creatinine concentration	51
13	Effect of MnO_2-NPs on urea concentration	51
14	Genotoxicity	52
15 (a, b)	Histopathological examination of liver	53
16 (a, b)	Histopathological examination of kidneys	54

ABBREVIATIONS

µm- micrometer

µmole- micromole

ANOVA- Analysis of Variance

CAT- Catalase activity

$MN0_2$-NPs - Manganese Dioxide Nanoparticles

N- Normality

nm-Nanometer

NM- Nanomaterials

DNA- Deoxyribonucleic Acid

DTNB- 5, 5'- dithiobis, 2-nitrobenzoic acid

Exp.- Experiment

Fig.- Figure

GSH- Reduced Glutathione

H_20- Water

H_2SO_4- Sulphuric Acid

HCl- Hydrochloric Acid

IU- Unit

Kg- Kilogram

M- Molarity

mg- milligram

mg- Milligram

g-Gram

MgCl2- Magnesium chloride

min- Minutes

mL-Millilitres

N- Normality

NaOH- Sodium Hydroxide

nm- Nanometer

NPs- Nanoparticles

NS- non-significant

pH- Potential of hydrogen

ROS- Reactive Oxygen Species

ALP- Alkaline Phosphatase

ALT-Alanine Transaminase

CAT-Catalase activity

SOD- SuperOxide Dismutase

GSH- Reduced Glutathione

ALB- Albumins

BIL- Bilirubin

GPx-Glutathione Peroxidase

DNPH-2,4-Dinitrophenylhydrazine

DTNB-5, 5-dithiobis, 2-nitrobenzoic acid

TCA-Trichloroacetic Acid

DW-Distilled Water

dl-decilitre

$FeCl_3$-Ferric chloride

H_2O_2- Hydrogen peroxide

$MgC1_2$- Magnesium chloride

OD- Optical density

pH- Potential of hydrogen

PCT-Proximal Convoluted Tubules

DCT- Distal Convoluted Tubules

DW- Distilled water

EXP-Experimental

Fig-Figure

b.w-Body Weight

ABSTRACT

The utilization of manganese oxide (MnO2) nanoparticles (NPs) in various industrial and biomedical applications has prompted concerns regarding their impact on human health and the environment. This study aimed to assess the toxicological implications of MnO2-NPs after 14 days of repeated oral administration in Swiss Albino Mice at two different doses (300 and 500 mg/kg b.w). Genotoxicity was evaluated using the comet assay. The results revealed a statistically non-significant increase in DNA damage following exposure to MnO2-NPs at both doses. Oral administration of MnO2-NPs induced mild alterations in biochemical, antioxidant, and histopathological parameters in mice. These findings contribute fundamental insights into the potential effects of MnO2-NPs through acute oral treatment.

Keywords: Biochemical parameters, oral toxicity, mice model, genotoxicity, MnO2-NPs, histopathology, oxidative stress, ROS, antioxidants

TABLES OF CONTENTS

CHAPTER 1: INTRODUCTION		
1.1	**Manganese: Properties, Biological roles and Applications**	**3**
1.2	**MnO_2 NP: Properties and Applications**	**4**
1.3	**Background/SOURCES**	**5**
1.4	**General Toxicity**	**6-10**
1.5	**Lacunae**	**11**
1.6	**Hypothesis**	**12**
1.7	**Objectives**	**12**
CHAPTER 2: LITERATURE REVIEW		**13-20**
CHAPTER 3: MATERIALS AND METHODS		
3.1	**Glassware**	**21**
3.2	**Instrumentations**	**21**
3.3	**Chemicals**	**21**
3.4	**Procurement of nanoparticles**	**21-22**
3.5	**Animal model: Mouse (Mus musculus) and maintenance**	**22-23**
3.6	**Experimental setup**	**23-24**
3.7	**General examinations**	**24**
3.8	**Euthanasia**	**24**
3.9	**Collection of tissue**	**24**
3.10	**Histology**	**24**
3.11	**Extraction and estimation of biomolecules and enzymes**	**25-38**

3.12	**Genotoxicity**	**38-40**
3.13	**Statistical Analysis**	**40**
CHAPTER 4: RESULTS		
4.1	**General Examination**	**41**
4.2	**Comet Assay**	**41**
4.3	**Histopathological Examinations**	**41**
4.4	**Effects of MnO_2-NPs on the biomolecules in the liver and kidney tissue**	**41-42**
4.5	**Effects of MnO_2-NPs on the liver enzymes**	**43**
4.6	**Effects of MnO_2-NPs on the antioxidants**	**43**
4.7	**Pearson's Correlation Analysis**	**44**
CHAPTER 5: DISCUSSIONS		**56-63**
CHAPTER 6: SUMMARY		**64**
6.1	**Conclusions**	**65**
6.2	**Future Scope**	**66**
CHAPTER 7: REFERENCES		**67**

1. INTRODUCTION

The 1980s marked the beginning of nanotechnology, which aimed to significantly enhance the ability to manipulate and visualize matter at the nanoscale (Contera et al., 2020). Today, nanotechnology is widely recognized as a rapidly evolving area of scientific research, with significant impacts across various industries and disciplines such as engineering, biology, chemistry, materials science, physics, pharmacy, and colloidal science (Malik et al., 2023).

As science and technology progress, researchers increasingly embrace technologies and products that are cost-effective, safe, and environmentally friendly compared to earlier methods. There is also growing concern about the financial viability of technologies due to the depletion of natural resources (Roco, 2011). Nanotechnology offers a solution to this challenge, presenting a safe, cleaner, and more affordable alternative to conventional methods (Singh, 2017).

Nanoparticles comprise a class of materials with dimensions in the 1–100-nm range that exhibit unique physical, chemical, and biological properties, making them distinct from their corresponding bulk materials or small molecules (Li et al., 2016; European Commission. Joint Research Centre., 2018). While theoretically nanoparticles can be created from a wide range of chemicals, the majority of nanoparticles currently utilized are derived from transition metals, silicon, carbon (including single-walled carbon nanotubes and fullerenes), and metal oxides such as zinc dioxide and titanium dioxide. In numerous instances, engineered nanoparticles are present as nanocrystals comprising various compounds like silicon and metals, known as quantum dots (Murray et al., 2000).

The unusual physicochemical properties of engineered NM are attributable to their small size (size, distribution and surface area), surface structure (inorganic or organic coatings, surface reactivity, surface groups, etc.), solubility, shape, chemical composition (electronic properties, purity, crystallinity, etc.) and aggregation making them highly desirable for various applications across commercial, medical, and environmental sectors (Masciangioli and Zhang, 2003; US Environmental Protection Agency, 2003). However, the same properties that make NPs appealing for advancement in nanomedicine and certain industrial applications could also prove to be detrimental when they interact with cells (Oberdörster, 2007). In 2014, 6214 organizations across 32 nations incorporated nanomaterials into 1814 consumer goods, with the majority (42%) falling within the health sector (Akçan et al., 2020).

NPs can be categorized into different nano systems depending on their composition, particle size, and morphology namely metallic, bimetallic or alloys, magnetic, polymeric, oxides, nanotubes, nanowires, nanoconjugates, crystalline, amorphous, so on (De Jesus et al., 2024).

Among the various nanomaterials designed, two-dimensional (2D) materials, especially transition metal dichalcogenides (e.g., MoS_2, WS_2, TiS_2, $MoSe_2$, and WSe_2) and transition metal oxides (TMOs, eg, MnO_2), have received a substantial amount of recent attention due to their widespread medical, consumer, industrial, and military applications. However, as particle size decreases, some metal-based NPs have shown increased toxicity, even if the same material is relatively inert in its bulk form (Schrand et al., 2010). Metal oxide NPs represent another industrially important class of nanomaterials**.** In recent years among the known metal oxides, manganese oxide NPs (especially, MnO_2) have attracted a lot of attention due to its unique properties (Hafez et al., 2019).

1.1 Manganese: properties, biological roles and applications

Manganese (Mn), a transition metal belonging to Group VIIB of the periodic table, exhibits oxidation states ranging from -3 to +7, with (MnO_2) or (Mn_3O_4) as the predominant form found in nature (Reidies, 2000). The physicochemical characteristics of manganese (Mn) closely mirror those of iron, making it an indispensable micronutrient needed for plant growth and for maintaining animals' health and well-being (Greenwood and Earnshaw, 1984). Mn plays pivotal roles in regulating the metabolism of macromolecules such as carbohydrates, lipids, and proteins, modulation of immune response, bone formation, free radical scavenging, and reproductive processes (Aschner & Aschner, 2005).

Tissues rich in mitochondria, including the liver, muscles, and brain shows an affinity for manganese (Mn), where it serves as an activator and cofactor for various metalloenzymes, such as the mitochondrial protein superoxide-dismutase (Mn-SOD), which plays a vital role in reducing oxidative stress arginase, involved in urea production in the liver, pyruvate carboxylase, essential for gluconeogenesis and glutamine synthetase, an astrocyte-specific enzyme that converts glutamate into glutamine. Moreover, other enzymes that depend on manganese (Mn) include oxidoreductases, transferases, hydrolases, lyases, isomerases, and ligases. Therefore, it is essential to carefully control Mn levels for ensuring homeostatic concentrations of this ion (Crossgrove and Zheng, 2004; Santos et al., 2012 Martinez-Finley et al., 2013).

As a critical raw material, Mn is widely used in a number of applications, including the global steel industry, in the production of aluminum alloys, and the development of Mn batteries, glass, ceramics, dyes, pigments, soil, food supplements, and medicine (Clarke and Upson, 2017).

1.1.1 MnO_2-NPs: Properties and Applications

Manganese oxide is a transition metal oxide and a P-type semiconductor, having a band gap of 3.3 -3.8 eV (Affrald et al., 2022). Manganese oxide (Mn-oxide) consists of variety of structures (nanorods, nanobelts, nanosheets (NSs), nanowires, nanotubes, nanofibers and compositions (MnO, Mn_5O_8, Mn_2O_3, MnO_2, and Mn_3O_4)), are simple to manufacture and possess a high degree of stability, which further broadens its applications in a diverse range of fields such as in energy storage (lithium-ion batteries (LIBs), medicine (drug delivery, ultrasound and magnetic resonance imaging (MRI)), catalysis, biosensors, in templates for the production of nanomagnetic, sorbing materials, portable power sources, solar cells, electrical appliances, sensory electrodes and semi-conducting thermistors, soil and wastewater treatment (Augustin et al., 2015; Hsu et al., 2016; Prasad, 2017; Ghosh, 2020).

Electrochemical and oxidative properties of Mn oxides pre-destine them to be used as a component of nanocomposites, sensitive to a broad range of compounds, such as MnO_2 based biosensors that can detect, i.e., α-glucosidase, glucose, or glutathione (GSH) in human blood or *Salmonella typhimurium*, a pathogenic bacterium, in food products (Lee et al., 2019; Hao et al., 2020). In addition, due to its multienzyme nature, MnO_2-NPs mimic the activities of catalase and superoxide dismutase concurrently serving as reactive oxygen species (ROS) scavengers (Liu et al., 2019; Wang et al., 2019).

Over the past decade, numerous researchers have focused on exploring the potential of utilizing threadlike nanosized MnO_2 particles for various practical purposes. This exploration became feasible with the advancements in nanotechnological fields like nano-optics, nanoelectronics,

pharmacology, chemistry, and (Hua et al., 2012) metallurgy, which directly influenced the increase in production volumes of nano disperse MnO_2, in the creation of matrixes for nanomagnetic materials and sorbents nano accelerators, semiconductor thermistors However, despite such promising applications, MnO_2-NPs can present certain hazards to the health and safety of people and cause serious socio-economic and ethical issues (Zaitseva & Zemlyanova, 2020).

1.2. BACKGROUND / SOURCES

In various environmental and occupational settings, manganese (Mn) in diverse oxidation states (II, III, or IV) is commonly found, existing as oxides, silicates, borates, carbonates, and sulfides (Ghosh, 2020). Exposure may occur in work settings during manufacturing processes or in non-manufacturing environments where consumers interact with the product, either through inhalation or ingestion of drinking water (Zaitseva et al., 2014).

Human exposure to NPs, primarily in occupational settings, occurs primarily through inhalation (McConnell et al., 2010). Handling metals, from ore extraction to final product manufacturing and disposal, represents a significant source of NPs exposure. At elevated temperatures, the metal fumes released in air are found sometimes reaching hazardous concentrations within the workplace environments (Máté et al., 2016). In such instances, various factors, including the route (oral/nasal), volume, and intensity of breathing, influence internal exposure or particle size dictates where in the human airways inhaled solids will be deposited (Zhang & Kleinstreuer, 2011).

Manufacturing plants involved in production processes of nanomagnetic, sorbing materials, nanocatalysts, and semi-conducting thermistors can become the source of nanopowder emission to air, water, and soil exposing the general public to drinking water and agricultural produce contaminated with nanodispersed manganese oxide (N.V. Zaitseva et al., 2013). In addition, Mn from parenteral intake, fuel additives, as an anti-knock gasoline (methylcyclopentadienyl manganese tricarbonyl), fungicides (e.g. maneb and mancozeb), Mn containing aerosol (dust, fume, mist), use of glass, paints, ceramic cosmetics, leather, firework, fertilizers, pharmaceuticals, potassium permanganate used for cleaning, bleaching, and disinfection purposes are some other ways, through which people can come into its contact (Sukmarani et al., 2020).

Other occupational settings include welding, mining, refining, production of ferroalloys, and steel or dry battery manufacturing etc. (Agency for Toxic Substances and Disease Registry [ATSDR], 2012). Numerous studies have also reported that Manganese oxide (MnO_2)- NPs used as contrast agents for magnetic resonance imaging (MRI), drug delivery, an ionization- assisting reagent in mass spectroscopy, waste water treatment and consumer products such as batteries, enhance the probable risk to occupationally exposed humans and the environment (Chen and He, 2008; Rutz, 2009; Shin et al., 2009; Taira et al., 2009).

1.3 GENERAL TOXICITY

Although Exposures to airborne nanosized particles (NSPs; < 100 nm) have been experienced by humans throughout the course of their evolution, it is not until the onset of the industrial revolution that such exposures have significantly escalated due to anthropogenic factors like internal combustion engines, power plants, and various sources of thermal-degradation. The rapidly

advancing field of nanotechnology is now set to introduce new routes of NSP exposure in humans, including inhalation (respiratory tract), ingestion (gastrointestinal tract), dermal contact (skin), and injection (blood circulation) (Oberdörster et al., 2005).

Potential occupational and public exposure to manufactured nanoparticles will increase dramatically in the near future due to the ability of nanomaterial to improve the quality and performance of many consumer products the public employs daily as well as the development of medical therapies and tests which will use manufactured NPs. To address ongoing debates and concerns, the field of nanotoxicology has arisen to investigate the toxicological effects of engineered NPs and ensure their safe utilization for both humans and the environment (Drobne, 2007).

As outlined in a report by the World Health Organization (WHO) in 2011, manganese (Mn) poisoning primarily affected individuals employed in mining and welding industries, where prolonged exposure to Mn-containing aerosols and dust is common, distinguishing them from the general populace, however cases of Mn toxicity have also been documented in individuals who consumed well-water contaminated with Mn or who were exposed to air pollution stemming from industrial emissions and fuel additives.

Manganese exhibits distinctive toxicity patterns, being largely harmless to adult organisms except for the brain, where inhalation of even moderate amounts over extended durations can induce symptoms resembling Parkinson's disease. Elevated manganese levels can also interfere with DNA replication and repair processes, resulting in DNA damage and abnormalities in mammalian cell chromosomes (Komura & Sakamoto, 1992).

With the recent development of nanomaterials, there have been several reports on the toxicity of NPs, stating their adverse effects on organs, tissue, cellular, sub-cellular and protein levels due to their unique physio-chemical properties (Schrand et al., 2010). Like other essential elements, Mn may induce toxicity under certain high-dose exposure conditions. Adverse neurological, reproductive, and respiratory effects characterize Mn toxicity in humans (Hussain et al. 2006; Limbach et al. 2007).

While humans regulate manganese (Mn) levels in tissues through precise control of absorption and excretion, excessive oral, parenteral, or ambient air exposure to Mn can result in its elevations in tissues (Aschner & Aschner, 2005). Manganese dioxide (MnO_2) nanoparticles exhibit an irregular shape, resulting in prolonged interaction with bodily tissues and reduced efficiency in being expelled from the body by the immune system's phagocytes through the lymphatic ducts (Gupta & Xie, 2018).

Lack of understanding regarding how nano-sized particles penetrate, localize, and induce morphological changes in organs and tissues upon entry into the body, emphasizes the necessity for conducting experiments to examine tissue structural alterations in internal organs. This is crucial for predicting and establishing safety standards for products containing nanoparticles (Schroeter et al., 2012)

Inhaling airborne particles containing manganese (Mn) poses significant health risks as Mn can quickly reach target areas before being excreted (Elder et al., 2006), leading to respiratory failure due to inflammatory changes and cell apoptosis in the lungs caused by MnO_2-NPs

which resist clearance mechanisms (Santos et al., 2012). MnO_2-NPs induce neurotoxicity by generating free radicals upon their interaction with cell membranes, leading to oxidative stress and cell death (Afeseh Ngwa et al., 2011; Horváth et al., 2012). Additionally, their high oxidative power disturbs testicular function, resulting in decreased sperm count, seminiferous tube diameter, and sperm motility in adult male mice (Yousefalizadegan et al., 2019).

In addition to oxidative stress, and inflammatory responses, it also leads to mitochondrial dysfunction, resulting in a significant increase in ROS production and oxidative stress indices, thereby reducing the levels of both enzymatic (superoxide dismutase [SOD], catalase [CAT], and glutathione peroxidase [GPx]) and nonenzymatic antioxidant levels (GSH and vitamin C) (Chtourou et al., 2013).

Given the fact that many researchers have recently reviewed the Mn-induced neurotoxicity (Harischandra et al., 2019), to the best of our knowledge, there is no comprehensive review existing regarding the toxicity of Mn on other vital organs such as spleen, liver, and kidneys. Also, despite the established routes of manganese excretion through hepatobiliary and renal pathways, limited information exists regarding manganese-induced hepatic and renal dysfunction (Sanchez-Gonzalez et al., 2015).

Oxidative stress also plays a significant role in manganese-induced liver damage and in the development and progression of nephrotoxicity. Manganese exhibits a strong attraction to sulfhydryl (thiol) groups present in proteins, as well as to reduced glutathione (GSH) and amino acids like cysteine (Chtourou et al., 2013). This interaction disrupts the antioxidant defense system

by inhibiting the functional SH groups. Therefore, maintaining balanced levels of redox metals is crucial for preventing tissue injury (Huang et al., 2011).

The liver serves as the central organ responsible for managing the storage, redistribution, and removal of manganese (Mn) to maintain a balanced Mn level in the body. Consequently, excessive exposure to Mn can cause significant harm to the liver, hindering the process of Mn elimination and potentially contributing to the development of chronic liver conditions (Crossgrove and Zheng, 2004; Michael et al., 2009).

The kidney plays a vital role in regulating fluid balance, filtering toxins, and metabolizing substances. It is among the major organs with high manganese (Mn) concentration, receiving around 5% of Mn from the bloodstream. While lower than the liver's deposition (30%), it surpasses that of the brain (0.1%). High Mn exposure, according to both in vivo and in vitro studies, leads to renal dysfunction, including various conditions like glomerulosclerosis, glomerulonephritis, and tubular damage (Chandel & Jain, 2016; Oladipo et al., 2016; Ismail, 2019; Niknahad et al., 2020).

Commonly observed mechanisms of NP toxicity involve oxidative stress and genetic harm, hence evaluating the genotoxicity of nanoparticles (NPs) is crucial for ensuring safety and monitoring environmental impacts, as it helps to identify potential mutations and cancer risks from exposure (Mangalampalli et al., 2018). The comet test is a sensitive technique for the measurement of DNA damage and alkali-labile sites in specific cells induced through different types of genotoxic agents (Tice et al., 2000).

The levels of enzymatic as well as non-enzymatic antioxidants such as Malondialdehyde **(**MDA),

a byproduct of lipid peroxidation, along with GSH, SOD and CAT, in addition to the liver function enzymes such as ALT, ALP and AST serve as indicators of protein status and indicate notable changes in liver and kidney function. Histopathological analysis is essential for identifying tissue structural changes due to nanoparticle exposure and assessing toxic effects (Mangalampalli et al., 2018).

1.4 LACUNAE

The gastrointestinal system serves as a significant point of entry for NPs in both humans and animals (Oberdörster et al., 2005). Moreover, many health risks associated with NPs entering the GI tract stem from accidental ingestion, which can occur through various means such as exposure in manufacturing industries, contact with nano-structured surfaces, or consumption of contaminated drinking water or food (Ahamed et al., 2011).

The toxicity of NPs is being addressed by a number of standardized approaches encompassing both in vitro and in vivo approaches as well as detailed genomic and biodistribution analyses (Schrand et al., 2010). While there are numerous accounts of manganese (Mn) toxicity resulting from inhalation exposure in humans, there are relatively few reports on manganism caused by water or dietary intake (Dorman et al., 2001). Today there is a growing interest in utilizing manganese oxide nanoparticles for various purposes such as a sorbent and catalyst in the comprehensive treatment of liquid radioactive waste, as well as a larvicide, pose a risk to public health, as there is a possibility for manganese oxide nanoparticles to enter surface water bodies via waste or treated water, which serve as sources of local drinking water, and also potentially contaminate agricultural crops with dispersed nano-sized manganese oxide particles (Zaitseva et al., 2014).

No studies have been reported regarding the acute toxicity of Manganese dioxide Nanoparticles (MnO_2-NPs) in Swiss Albino Mice (*Mus musculus*) strain, via the oral gavage route. Therefore, in the present study Manganese dioxide nanoparticles (MnO_2-NP) will be administered in 2 different doses through oral gavage exposure method to study its acute effects on mice.

1.5 HYPOTHESIS

"Exposure to manganese dioxide nanoparticles (MnO_2-NPs) will result in biochemical and morphological changes in the liver and kidneys of Swiss Albino mice (*Mus musculus*)".

1.6 OBJECTIVES

1. To evaluate the effect of MnO_2-NPs on the kidney and liver functioning via various biochemical tests.
2. To evaluate the structural changes in the liver and kidney of mice (*Mus musculus*), via histological analysis.
3. To analyze oxidative stress biomarkers and genotoxicity.

2. LITERATURE REVIEW

Nanomaterials have surfaced as prominent candidates for numerous biomedical applications. Thus, for their future clinical implications, Numerous studies have been conducted to assess the toxicity of manganese nanoparticles, employing both in vitro and in vivo approaches (Mukherjee & Patra, 2016)

In vivo studies play a crucial role in assessing the toxicological effects of NPs due to the intricate nature of animal systems. These studies investigate interactions between NPs and biological systems, revealing potential novel immune responses, metabolic patterns, biodistribution, and clearance mechanisms. Such findings provide valuable insights for assessing potential health hazards in humans (Fischer and Chan, 2007).

Sárközi et al. (2009) found that manganese oxide nanoparticles due to their small size and high penetrating capacities can penetrate through the blood-brain barrier and even small concentrations regardless of the route of entry can cause morpho functional disruptions of various parts of the central nervous system.

Once nanoparticles are absorbed, they have exceptional mobility within the body of animals or humans can cross conventional barriers such as the alveolar or capillary wall. This ability, along with the inflammatory nature of nanoparticles, is greatly impacted by their surface properties, as reported by (Ryman-Rasmussen et al., 2007).

According to Lison et al. (1997) MnO_2 nanoparticles, characterized by their non-spherical shape, are known to be excreted from the body at a slower rate by the immune system's phagocytes via lymphatic ducts, resulting in prolonged contact with bodily tissues.

Several researchers have directed their attention in evaluating the potential risks associated with the impact of manganese oxide nanoparticles, primarily focusing on the inhalation route as the most likely pathway of entry into the human body (Sakon, 2003; Frick et al., 2011). Their findings have demonstrated that the inhalation intake of manganese oxide nanoparticles can lead to adverse and toxic health effects, including an active catalytic generation of reactive oxygen species (ROS) observed in alveolar epithelial cells of humans after 24 hours of exposure, and an increase in the levels of extracellular and intracellular oxidized forms of glutathione by 30 and 80%, respectively.

Based on the study conducted by Elder et al. (2006), it was reported that manganese oxide nanoparticles (IV) sized less than 30 μm, when administered via inhalation, can penetrate PC-12 neuron-like cells of the cerebrum via the olfactory nerve, and accumulate in the astrocytes of cerebrum cells. This process is accompanied by a slight inhibition of mitochondrial activity and a dose-dependent decrease in the concentration of dopamine and its metabolites, dihydroxyphenylacetic acid and homovanillic acid.

The clinical presentation of acute intoxication, described in previous studies, proved that nanosized MnO_2 particles have the ability to induce neurotoxic effects and respiratory failure, ultimately leading to mortality in the studied animals. The impact was notably more significant in the case of nano-dispersed particles compared to the micro-dispersed counterparts, primarily due to the heightened specific surface area of nanoparticles, which facilitates the active generation of free radicals upon interaction with the bilipid layer of cellular membranes. The progression of

respiratory failure was also associated with the tested nanoparticles' potential to provoke inflammatory responses, resulting in the apoptosis of alveolar epithelial cells. Additionally, MnO_2 nanoparticles exhibited increased resistance to mucociliary clearance, thereby prolonging their interaction with respiratory epithelial cells compared to the micro-disperse analogs (Sárközi et al., 2009; Afeseh Ngwa et al., 2011; Zvezdin et al., 2015).

According to Tseng et al. (2012) and Chen et al. (2013), one of the pronounced effects associated with the intake of nanoparticles of a number of metals and nonmetals is hepatotoxicity, the symptoms of which include changes in enzyme activity, apoptosis activation and fine structure changes of the hepatocytes and Kupffer cells.

Studies have indicated that magnetic nanoparticles exhibit biosafety and compatibility within living organisms, making them suitable for biomedical applications. Nonetheless, toxicological assessments have uncovered negative health impacts of magnetic nanoparticles on both humans and other living organisms. The biological safety of MnO_2 nanoparticles continues to be a subject of debate (Mahmoudi et al., 2012).

N.V. Zaitseva et al. (2013) explored the adverse effects of both nano dispersed and micro-sized manganese oxide (III, IV) particles following intragastric administration in Wistar rats over a 30-day period. The study revealed a reduction in body weight, activation of oxidation processes, decline in antioxidant capabilities, impairment of hepatocyte membranes, and abnormalities in the hepatic function responsible for protein synthesis. Furthermore, it was suggested that exploration in this field is essential to clarify the mechanisms behind these noted impacts and to provide

insights for safety assessments regarding potential human contact.

Singh et al. (2013) conducted a study with the aim of examining the health and safety implications of manganese oxide nanoparticles (MnO_2-NPs) and microparticles (MnO_2-MPs) by conducting various toxicity assessments in Wistar rat. The primary objective was to investigate oral toxicity, genotoxicity, biochemical changes, histopathological alterations, and tissue distribution of these particles over a 28-day period. Their investigation revealed that prolonged exposure to MnO_2 particles could induce genetic damage, biochemical shifts, and histological modifications, highlighting the importance of addressing health and safety concerns associated with nanomaterials in order to mitigate potential risks.

Sedigeh et al. (2014) investigated the effects of prolonged subcutaneous exposure to nano- and microparticles of manganese dioxide (MnO_2) on the liver, kidneys, and testes of rats. Results showed that administration of MnO_2 nanoparticles led to more severe tissue damage compared to an equivalent dose of MnO_2 microparticles in all examined tissues, indicating that reduction in particle size from micrometers to nanometers appeared to amplify the adverse effects of these particles on the tested tissues.

Several studies have reported that a primary driver of Mn-induced cellular toxicity and organ impairment stems from the generation of reactive oxygen species (ROS) and subsequent oxidative stress induced by nanoparticles, particularly those composed of metal oxides. Elevated levels of ROS can cause harm to various macromolecules such as DNA, proteins, and lipids, while also depleting antioxidant reserves, triggering apoptosis by damaging mitochondrial membranes, and contributing to the onset of conditions like cancer and neurodegenerative diseases, (Manke et al.

2013; Fu et al. 2014).

In 2014, Zaitseva and colleagues analyzed the effects of sub chronic exposure to MnO nanoparticles on peroxidation and antioxidant status in the central nervous system (CNS) of rats. Their results indicate that MnO nanoparticles facilitate lipid peroxidation and suppress antioxidant enzyme activity, leading to neurotransmitter imbalances and morphological changes in brain tissues.

Limbach et al. (2007) showed that manganese (II, III) oxide nanoparticles (Mn_3O_4-NPs) cause generation of reactive oxygen species (ROS) in human lung cancer cells (A549).

Frick et al. (2011) investigated the toxicity of manganese oxide nanoparticles on rat lung cells compared to soluble manganese salt and other metal oxide nanoparticles. The researchers found that manganese oxide nanoparticles caused oxidative stress, increased cell death, and showed catalytic activity. These nanoparticles generated reactive oxygen species, oxidized intracellular glutathione, and were taken up by the cells. The nanoparticles' catalytic activity and ability to penetrate cell membranes contributed to their toxicity, leading to cell death. In contrast, the soluble manganese salt triggered cell death through different mechanisms.

Gandhi et al. (2022) highlighted the dual nature of manganese (Mn) as both an essential trace element for humans and a potential toxin when exposure levels exceed certain thresholds. The discusses how Mn exposure can lead to various health problems, particularly neurological abnormalities, but also potentially affecting multiple organ functions such as the lung, liver, and kidney, and the various mechanisms underlying Mn toxicity, including oxidative stress, apoptosis, and inflammatory responses and also examines sources of Mn exposure, absorption, distribution

in different organs, and available treatment strategies.

The antioxidant properties of various manganese oxide nanoparticles (NPs), were explored by Tootoonchi et al. (2017), with the aim to assess the biocompatibility and safety of nano-sized manganese oxides. MnO_2-NPs displayed protective qualities against cells subjected to H_2O_2 for 6 hour. The antioxidant capabilities were more pronounced at increasing NP concentrations, up to 50 µg/mL, after which they decreased, suggesting potential depletion of the redox system. These findings indicate that nano-sized manganese oxides may possess biocompatible and safe properties, with potential antioxidant benefits under certain conditions.

In a different study, Feng et al. (2018) focused on exploring the magnetic targeting and tumor microenvironment response using magnetic nanoconjugates containing an iron carbide–glucose oxidase–manganese nano shell. The researchers aimed to assess the clearance and toxicity of these nanoparticles after intravenous injection in mice. Results revealed a time-dependent clearance, particularly via the kidney and liver, with no pathological abnormalities observed in major organs such as the liver, spleen, heart, kidney, and lung, while biochemical assays indicated normal liver function based on the levels of alanine aminotransferase (ALT), alkaline phosphatase (ALP), and aspartate aminotransferase (AST). remained normal, indicating the biocompatibility and safety of the magnetic nanoconjugates, supporting their potential for targeted therapy applications.

Zhou et al. (2018) reported the clearance of manganese nanoparticles through the renal route. They developed and synthesized small manganese and gallium-doped copper sulfide nanodots using

bovine serum albumin (BSA) as a template for triple modal imaging and photothermal therapy. Results from imaging systems confirmed efficient clearance via the renal urinary route, thereby reducing toxicity to non-tumor organs.

Xu et al. (2017) synthesized manganese–melanin nanoparticles as MRI contrast agents for in vivo tumor targeting. Further, the authors claimed that these nanoparticles were found to be less toxic than the clinically approved MRI agent Gadodiamide. The manganese–melanin nanoparticles were also cleared from the body via the hepatobiliary and renal system, proving to be less toxic to the body organs with specific tumor targeting capability.

The biocompatibility of manganese dioxide (MnO_2) nanosheets, with a thickness of 2 nm, modified with soybean phospholipid in Kunming mice was investigated following intravenous administration of nanoparticle suspension at varying doses (5, 10, and 20 mg/kg). No signs of inflammation or fibrosis were observed in major organs such as the kidneys, heart, lung, liver, or spleen, even after a thirty-day period. Additionally, there were no significant differences in body weight, indicating the nanoparticles' lack of adverse effects (Liu et al., 2019).

On the other hand, Mn_3O_4-NPs coated with PEG (10 ± 2.3 nm), designed as an MRI contrasting agent, showed good biocompatibility after intravenous injection in mice (20 mg/kg). Two weeks post-exposure, no discernible histopathological alterations were observed in major organs including the lungs, heart, spleen, liver, or kidneys, when compared to the control group. Biochemical markers reflecting liver and kidney functions, such as alkaline phosphatase, total bilirubin, serum creatinine, and serum urea, exhibited no significant changes. Although levels of ALT and AST experienced slight decreases, they remained within the normal physiological range

(Zhan et al., 2018).

Manganese oxide nanoparticles (60 nm) were modified with PEG-Cy5.5 to improve MRI contrast and serve as a drug delivery system, were administered intravenously to C57BL/6J mice at a dosage of 35 mg/kg body weight. Following a 28-day period, there were no observed alterations in behavioral patterns such as eating habits or exploratory activity. Histopathological examination of various organs including the heart, liver, spleen, kidney, lung, and brain showed no discernible changes (Zheng et al. 2018).

3. Materials and Methodology

3.1 Glassware

General laboratory glassware including volumetric flask, measuring cylinders, beakers, mortar and pestle, glass rod, test tubes, plastic and glass reagent bottles were used. All the glassware was soaked in 4% chromic acid overnight. All the glassware was rinsed with distilled water and sterilized by keeping in a hot air oven before use**.**

3.2 Instrumentation

Weighing balances (Wensar PGB 200), water bath, pH meter (TOSHCON TMP3), Vortex (CM 101), Refrigerator, Deep freezer (-20°C), Centrifuge (REMI R-24), hot air oven (MIC-165), light microscope (Olympus, BX53) Colorimetric spectrophotometer, used in the study are available in the Zoology Discipline, Goa University. Microtome for histology was utilized from Ashwini Pathological lab.

3.3 Chemicals

The chemicals used were of Analytical Grade from Thermo-fisher, Sigma- Aldrich, Hi-media, Merck etc.

3.4 Procurement of the nanoparticles

Manganese dioxide Nanoparticles (MnO_2-NPs) with a molecular weight of 86.9368g/mol was synthesized by my research guide and its specifications and protocol is as follows:

- APPEARANCE- Black powder (Solid).

- PURITY- 99%.
- RELATIVE DENSITY- 5.026 g/cm3.

The MnO_2 nanostructures were synthesized via a wet chemical redox method as detailed by Naik et al. (2021). Briefly, analytical-grade $KMnO_4$ and $MnSO_4.H_2O$ were mixed in a 2:3 ratio, heated, and stirred. Dropwise addition of $KMnO_4$ to the heated $MnSO_4$ solution resulted in the formation of a brownish-black precipitate, indicating the formation of hydrated MnO_2 nanoparticles, which were then filtered, washed, and dried. The XRD pattern of the nanostructure revealed that the compound is α-MnO_2 (Hollandite). SEM images depict a sea-urchin-like morphology with spike-like structures, indicating a high surface area. TEM images validate this morphology, showing fine spike-like structures with varying dimensions and poor crystallinity in the Electron Diffraction pattern, attributed to lower heating conditions.

3.5 Animal model: Mouse (*Mus musculus*) and maintenance.

Mice are frequently used in research due to their close resemblance to humans in terms of anatomy, physiology, and genetics. Additionally, their small size, short reproduction cycle and lifespan, affordability, and widespread availability make them advantageous for experimentation (Hickman et al., 2017). A total of 15 healthy male Swiss Albino Mice (*Mus musculus*), 6-8 weeks of age having average body weight of 28-30g, were obtained from National Institute of Biosciences, Pune, India. The necessary ethical approval was acquired from the Animal Ethics Committee of Goa University (Ref no.GUZ/IAEC/23-24/N2, dated 12/09/2023) for the use of these animals prior to the start of the experimentation.

All 15 Male Swiss Albino Mice (*Mus musculus*), were kept and maintained at the animal house facility of the Department of Zoology, Goa University by strictly following the CPCSEA guidelines throughout the study period. After the initial acclimatization for a period of one week, animals of uniform body weights i.e., 28-30 g were selected for the present study. The mice were housed in polypropylene cages with stainless steel lid, having provision for food and water. They were given standard bedding containing sawdust which was replaced twice a week to maintain hygiene. The animals were maintained at ambient laboratory conditions (Temp = 21±0.6°C, 63+5% humidity and 12h dark-light cycle) and fed with commercial diet and tap water provided ad libitum (Tulinska et al., 2020).

Table No. 1 DOSE CONCENTRATION

Groups	No.of individuals in each group	Doses (mg/kg) b.w	Vehicle of administration
CONTROL	**5**	**-**	**Distilled water**
EXP. GROUP 1	**5**	**100 mg/kg b.w**	**0.9% Physiological Saline**
EXP. GROUP 2	**5**	**500 mg/kg b.w**	**0.9% Physiological Saline**
TOTAL	**15**		

3.6 Experimental setup

Once the mice were acclimatized, they were randomly assigned into 3 groups, each comprising of 5 individuals each [i.e., 2 experimental and 1 control group]. MnO2-NPs with different concentrations (100 mg/kg b.w and 500 mg/kg b.w) were suspended in physiological saline, properly ultrasonicated (UP100H; Hielscher Ultrasonic, Gumby, Germany) and vortexed before every treatment of the mice and fed once daily to the mice of the experimental groups for 14 days

(Naser et al., 2020) while the mice in the control group were fed only with distilled water (Sulaiman et al., 2015) (Table no.1).

3.7 General examination

For a period of 14 days, the mice were routinely examined for their survival, behavioral changes such as rolling of tail, hyperactivity, drowsiness, overfeeding, isolation, motor impairments and morphological changes in hair, skin texture and color.

3.8 Euthanasia

After 14 days of exposure, all the animals were sacrificed by cervical dislocation. The procedure involves the dislocation of the spinal column from the neck/brain by applying pressure.

3.9 Collection of tissue

After sacrificing and dissecting the mice, the liver and kidneys were removed and washed with physiological saline, and weighed quickly. The tissues used for biochemical estimations were stored at -20°C until further use.

3.10 Histology

Kidney and liver for histological examination were washed thoroughly with physiological saline, weighed and stored in 10% formalin. After dehydration with 70% alcohol, the samples were embedded in paraffin wax and six-micron thick sections were prepared and stained with hematoxylin and eosin. The prepared slides were further analyzed at 20x under a light microscope (Olympus BX53) and images were captured using ProgRes software (Olympus).

3.11. Extraction and estimations of Biomolecules and Enzymes.

3.11.a. Preparation of tissue homogenate.

After the animals were sacrificed, the liver and kidneys were washed thoroughly and rinsed with 0.9% physiological Saline. They were gently blotted between the folds of a filter paper and weighed in an analytical balance. 10% of homogenate was prepared in 0.01 M phosphate buffer (pH 7) using a polytron homogenizer at 4'C. The homogenization was done in a cold chamber set at 4°C. The homogenates were then centrifuged at 3000 rpm for 15-20 min. The resulting supernatants were stored at -4° C in clean sterile microcentrifuge tubes until analysis.

3.11.b. Assays for metabolites

A] Estimation of Total Proteins [Lowry et al., 1951].

Principle:

Peptide bonds (-CO-NH-) within proteins react with copper [II] ions in alkaline conditions, leading to the reduction of the Folin-Ciocalteau reagent. This reagent contains a mixture of sodium tungstate, sodium molybdate, and phosphate, resulting in bluish-colored products. The intensity of the colour, ranging from blue to purple, is indicative of the concentration of aromatic amino acids such as tryptophan and tyrosine, which undergo copper-catalyzed oxidation to form hetero-polymolybdenum blue.

Reagents Required:

1. Reagent A: 2% sodium carbonate in 0.1 N sodium hydroxide.
2. Reagent B: 0.5% copper sulphate (CuSO4.5H2O) Prepare fresh by mixing stock solutions.
3. Reagent C: 1% potassium sodium tartarate. Prepare fresh by mixing stock solutions.
4. Alkaline copper solution (Reagent D): Mix 48mL of reagent A and 1 mL of reagent B

and 1 mL of Reagent C prior to use.

5. Diluted Folin's reagent (Reagent E): Dilute Folin-Ciocalteau reagent with an equal volume of 0.1 N NaOH

6. Standard: Dissolve 10 mg BSA in 40mL of distilled water in a volumetric flask. Take 10mL of this stock standard and dilute to 50 mL in 0.1N NaOH. .

Protocol:

0.1ml of the tissue extract for protein was diluted up to 0.5 ml with distilled water to which 5 ml of Lowry's reagent was added and incubated for 15 minutes at room temperature. Then 0.5ml of Folin Cio-Calteau (1:2 dilution) reagent was added and kept for a further incubation period of 30 minutes. The blue- coloured complex intensity was measured against a suitable blank at 690 nm (Lowry et al., 1951). Quantification of the protein content of the sample was done with the help of a standard curve of bovine serum albumin (200ug/ml BSA in 0.1N NaOH).

B] Albumins [Godkar, 1994].

Principle:

At pH 4.1, the Albumin present in the sample binds specifically with bromocresol green (BCG) to form green colored complex, the intensity of which is measured colorimetric ally at 640nm and is directly proportional to the concentration of albumin present in the given sample. The pH is maintained during the reaction by a buffer.

Reagents Required:

Albumin reagent: 8.85g succinic acid, 0.108g of bromocresol green, (0.1g of sodium azide, and 4.0 ml of Triton-X 100 were dissolved in 900 ml of distilled water. The pH of this solution was adjusted to 4.1 by using IN sodium hydroxide. The final volume was made up to 100 ml by using distilled water.

Protocol:

100ul of tissue protein extract was mixed with 5ml of albumin reagent. The mixture was incubated at room temperature for 10 minutes. The intensity of the color was measured at 640nm against a suitable blank (Godkar, 1994). Albumin present in the samples was quantified with the help of the albumin standard curve (4.0g/dl prepared in 0.1g/dl sodium azide).

C] Bilirubin [Malloy & Evelyn, 1937].

Principle:

Bilirubin and bilirubin glucuronate react with diazotized sulfanilic acid (Ehrlich's Reagent), and is converted to azobilirubin molecules which give a red purple color in acid, the intensity of which is read colorimetric ally at 540 nm.

Reagents Required:

1. Diazo reagent: Make freshly before use the mixing 10 ml of solution A and 0.3ml of solution B. Solution A: 1g of sulphanilic acid and 15 ml of concentrated HCL per liter in water.
Solution B: 0.5g of sodium nitrite/100ml in water. This solution should be kept in refrigerator renewed monthly.

2. Diazo Blank: 15 mL of conc. HCL/liter in water.

3. Methanol

4. Bilirubin standard: Dissolve 10 ml of 10mg% bilirubin in a minimum (about 5ml) of 0.1N sodium solution.

Protocol:

0.1ml of serum was diluted with 1.8 ml of distilled water. 0.5 ml of the Diazo Reagent and 2.5 ml of Methanol was mixed and allowed to stand in dark for 30 min. The absorbance was read at 540 nm using distilled water as blank.

D] Total carbohydrates [Carroll et al., 1955].

Principle:

Carbohydrates are dehydrated by conc. H2SO4 to form hydroxymethyl furfural. Furfural condenses with anthrone to form a blue colored complex, which can be measured colorimetrically at 620 nm.

Reagent Required:

Anthrone reagent: 0.2gm of anthrone was dissolved in 100ml of concentrated sulphuric acid.

Protocol:

To 0.1ml of deproteinized aliquot, 5 ml of Anthrone reagent was added and then the mixture was incubated for 10 minutes in boiling water bath. The intensity of the color developed was measured at 620 nm against a suitable blank (Carroll et al., 1955). Quantification of the total carbohydrate content was done with the help of a standard curve of total carbohydrate (100pg of glucose/ml).

E] Free sugars [Nelson, 1944].

Principle:

When sugars are heated with an alkaline copper reagent, they generate cuprous oxide, which forms a blue-coloured complex on reacting with arsenomolybdate reagent, and the intensity of this complex can be measured at 540 nm.

Reagents Required:

1. Alkaline copper reagent: A] a)- 12.0g anhydrous sodium carbonate and 6.0g sodium potassium tartrate were dissolved in 125 ml of distilled water. b)-2.0 g of copper sulphate was dissolved in 25 ml distilled water. Both the solutions a and b were mixed, 8.0g of sodium bicarbonate was added to it by stirring to prepare solution A.

B] 90.0g of anhydrous sodium sulphate was dissolved in 250 ml of distilled water. Boiled to expel

air and then cooled to room temperature to prepare solution B. Now both the solutions A and B were mixed and the volume was made up to 500ml with distilled water.

2. Arsenomolybdate colour reagent: 25.0 g of ammonium molybdate was dissolved in 450 ml of distilled water. 21m1 of concentrated sulphuric acid was added slowly while mixing. To this, 3.0 g disodium hydrogen arsenate (already dissolved in 25 ml of water) was added. Mixed well, stored in amber coloured bottle at 37°C for 48 hours.

Protocol:

To 1.0 ml deproteinized sample, 1.0 ml alkaline copper reagent was added and incubated in the boiling water bath for 20 minutes. After cooling to room temperature 1 ml of arseno-molybdate colour reagent was added. The mixture was diluted with 7 ml distilled water. The intensity of the colour was read at 540 nm against a suitable blank (Nelson, 1944). Quantification of tissue free sugar concentration was calculated with the help of glucose standard curve, prepared by using 200 µg/ml-glucose as a standard solution.

F] Urea [Friedman, 1953].

Principle:

Urea reacts with diacetyl monoxime in hot acidic medium, in the presence of ferric ions, resulting in the formation of a pink-coloured substance called diazine. Thiosemicarbazide and ferric ions are added to enhance the reaction and increase colour intensity, which can be measured at 520 nm.

Reagents Required:

1. Acid mixture: 10.0mg of ferric chloride was dissolved in 100ml of orthophosphoric acid,

2. Diacetyl monoxime reagent: 2.5g of diacetyl monoxime and 0.12g of thiosemicarbazide was dissolved in 100ml distilled water.

Protocol:

0.1ml of serum was diluted up to 3 ml with distilled water. 2ml of the acid mixture and 0.2 ml of diacetyl, monoxime reagent were added. It was then incubated in a boiling water bath for 20 mins and then cooled at room temperature. The intensity of colour was measured at 530 nm. The amount of urea present in various samples was calculated using standard curves of urea 10µg/ml.

G] Creatinine [Brod and Siruta, 1948].

Principle:

Creatinine in alkaline medium reacts with picric acid to form a Yellow-red tautomer of creatinine intensity of which is measured at 520 nm in a spectrophotometer.

Reagents Required:

1. Alkaline picric acid: it is prepared fresh by mixing four parts of picric acid and one part of sodium hydroxide. This working reagent is stable for one day.
2. Creatinine standard solution: Dissolve 100 mg creatinine in 100 ml of water. Working standard solution may be prepared by appropriate dilution of the stock solution.

Protocol:

The supernatant was collected and 2 ml alkaline picric reagent was added. The contents were mixed thoroughly and were kept at room temperature for 20 minutes. The intensity of colour was measured at 520mm. Quantification of serum creatinine was done with the help of a standard curve creatinine.

3.11.c. Assays for antioxidants

A] Catalase [Sinha, 1972].

Principle:

Catalase causes rapid decomposition of hydrogen peroxide to water.

$H2O_2$ — $H_2O + O_2$

The reduction of dichromate to chromic acetate in acetic acid when heated with H_2O_2, leads to the formation of unstable perchloric acid as an intermediate. Chromic acetate is then measured at 610 nm using colorimetry. Since dichromate has no absorbance in this region, the presence of the compound in the assay mixture do not interfere with the colorimetric determination of chromic acetate.

Reagents Required:

1. 0.01 M Phosphate buffer, pH 7.0
2. 0.2 M Hydrogen peroxide
3. Dichromate acetic acid reagent: 5% potassium dichromate and glacial acetic acid were taken in a 1:3 ratio.
4. Working catalase standard: Take 0.1ml of prepared standard and dissolve in 9.9 ml of D.W

Protocol:

1.5 ml of phosphate buffer (0.01 M, pH 7.0) and 0.4 ml of the substrate (0.2 M H2O2) were taken and incubated at 37°C for 5 minutes. 0.1 ml phosphate buffer was added to prepare the enzyme blank and 0.1 ml serum or tissue homogenate was added to assay the enzyme activity. This reaction mixture was incubated at 37°C for 15 minutes. The reaction was stopped by the addition of 2.0 ml of dichromate acetic acid reagent. The solution was then heated in a boiling water bath for 10 minutes, mixed well and the intensity of the colour was measured against a reference blank at 620 nm. (Protein content in the enzyme was estimated as described earlier. The enzyme activity was quantified with the help of a reference curve of catalase enzyme (0.25g/5ml) and expressed as mg/ml of consumed protein.

B] Superoxide Dismutase (SOD) [Beauchamp and Fridovich, 1971].

Principle:

Nitro blue tetrazolium chloride (NBT) reacts with superoxide anions generated by riboflavin under light in the presence of methionine, forming a blue-coloured compound called formazan. Superoxide dismutase in the sample reduces the superoxide anions, resulting in less formazan production and decreased blue colour intensity. The reduction in formazan formation correlates directly with SOD concentration. A 50% decrease in formazan formation represents one unit of SOD.

Reagents Required:

1. Potassium Dihydrogen phosphate
2. Di potassium hydrogen phosphate
3. Nitroblue tetrazolium chloride
4. Riboflavin
5. Methionine
6. SOD substrate-To 25ml of 0.2M potassium phosphate buffer (pH 7.0), 149 mg of methionine, 4.93ml of nitroblue tetrazolium chloride (1mg/ml in 50mM potassium phosphate buffer, pH 7.0) and 0.63ml of riboflavin (1 mg/ml in 0.05M potassium phosphate buffer) were added and the volume was made up to 100 ml with double distilled water.

Protocol:

To 2.9 ml of freshly prepared SOD substrate, 0.1 ml of serum or liver tissue homogenate (5% homogenate was prepared in ice cold 10mM of potassium phosphate buffer, pH 7.0, and it was brought down to 2.5% with 50 mM potassium phosphate buffer, pH 7.0 and then centrifuged. The clear supernatant was used for the assay) was added. Enzyme blank was' prepared by adding 0.1

ml 50 mM potassium phosphate buffer, pH 7.0 instead of sample. Illumination was carried out in the aluminium foil lined box fitted with a 15 V fluorescent lamp for exactly 10 minutes. The reaction was stopped by switching off the source of illumination. Intensity of the colour was read at 560 nm (Beauchamp and Fridovich, 1971). Enzyme activity was quantified with the help of a standard curve of SOD (400ug/ml). Protein content in the enzyme was estimated as described earlier (Section 4.1.3 A). SOD activity was expressed as IU/mg protein. One unit of the enzyme can be defined as the amount of SOD required to inhibit 50% of NBT reduction at standard condition

C] Thiobarbituric Acid Reactive Substances (TBARS) [Niehaus and Samuelsson, 1968].

Principle:

Malondialdehyde forms a 1:2 adduct with thiobarbituric acid to produce a coloured complex. The intensity of the colour was measured spectrophotometrically at 535 nm. Other lipoproteins are precipitated out by trichloroacetic acid and avoided from interfering in the reaction. Only water-soluble malondialdehyde reacts with thiobarbituric acid and produces a coloured complex.

Reagents Required:

1. TBA-TCA-HCI Reagent: 0.37% Thiobarbituric acid, 15% Trichloroacetic acid and 0.25(N) Hydrochloric acid were mixed in a 1:1:1 ratio to prepare this reagent.

2. Working MDA standard: Take 0.1 ml of the prepared standard and dissolve in 9.9 ml of D.W

Extraction:

The liver tissue was homogenised in Tris HCl buffer pH 7.0 at 1500 rpm for 10 min.

Protocol:

0.1 ml of tissue homogenate or 10 µl serum was treated with 2m1 of TBA-TCA-HCI reagent and placed in a boiling water bath for 15 minutes, cooled and centrifuged at room temperature for 10 minutes at 500 x g. The absorbance of a clear supernatant was measured against a suitable blank at 535 nm (Niehaus and Samuelsson, 1968). Thiobarbituric acid reactive substance concentration was estimated with the help of a standard curve of malondialdehyde (0.627g/20 ml of glacial acetic acid).

D] Reduced Glutathione (GSH) [Hemmadi, 2016].

Glutathione, a tripeptide, shows varying intracellular levels that varies with the growth, nutritional state, and hormonal balance. Tissues like the mammalian liver typically have abundant reduced glutathione. It functions as an antioxidant and exists in two forms: reduced (GSH) and oxidised (GSSG). The sulfhydryl (thiol) group in reduced glutathione (GSH) acts as a proton donor and is responsible for its biological function.

Principle

The acid soluble sulfhydryl groups (non-protein thiols of which more than 93% is reduced glutathione) reacts with 5, 5- dithiobis, 2-nitrobenzoic acid (DTNB) to form a stable yellow coloured complex. The absorbance of the coloured complex can be measured spectrophotometrically at 412 nm.

Reagents Required

1. M-phosphoric acid (HPO_3 and $NaPO_3$).
2. Sodium chloride (NaCl).
3. Ethylene diamine tetra acetate (EDTA)-($C_{10}H1_6N_2O_8$).

4. 0.3M Di sodium hydrogen phosphate (Na_2HPO_4).

5. 5, 5'-Dithiobis (2 nitro benzoic acid) (DTNB) - ($C_{14}H_8N_2O_8S_2$): 40mg DTNB per 100mL of phosphate solution.

6. Reduced Glutathione Standard (100µg/mL).

Precipitating Solution:

1.67g of glacial m-phosphoric acid (A mixture of HPO3 and NaPO3), 0.2g disodium or dipotassium ethylene diamine tetra acetic acid (EDTA) and 30g of NaCl per 100mL of distilled water. The mixture may contain suspended fine precipitate of EDTA, which may not interfere, but added just to avoid the errors caused by metal ions in the preparations. This solution is stable for approximately 3 weeks at 40C.

Protocol:

The diluted samples are treated with 1.5ml of precipitating solution and kept for 10 minutes for the precipitation to complete. The solutions are then filtered through a Whatman No.1 filter paper. 500µl of the filtrate is taken and to this 2ml. of phosphate solution and 250µl of DTNB solution is added Simultaneously a blank is maintained containing 200µl of distilled water, 300µl, of precipitating solution, 2 ml of phosphate solution and 250µl of DTNB. The intensity of the yellow colour formed is spectrophotometrically read immediately (within ten minutes) at 412 nm against the blank. The optical densities obtained are plotted against the standard graph.

3.11.d. Assays for liver function enzymes

A] Alkaline phosphatase (ALP) [King and Armstrong, 1934]. Principle:

The amount of oxaloacetate or pyruvate produced by transamination is reacted with 2,4 dinitrophenyl hydrazine (DNPH) to form a brown-coloured hydrazone, the colour of which in

alkaline solution is read at 520 nm.

Reagents Required:

1. ALP Substrate - 0.375g glycine + 0.166 g NaOH + 0.01g MgCl2 + 0.165g p-nitro phenyl phosphate to 100ml. Maintain pH at 9.2

2. ALP Standard -250mg/mL of p-nitrophenol.

Protocol:

A 2.7 ml of glycine buffer was added with 0.2 ml of the substrate (freshly prepared) and incubated at 37°C for 5 minutes. To this 0.1 ml of 5% tissue, the homogenate was added to assay the enzyme activity. An enzyme blank was prepared by mixing 2.7 ml buffer, 0.2 ml substrate, and 0.1m1 of distilled water simultaneously. The reaction mixture was incubated at 37°C for 15 minutes and the reaction was stopped by adding 5 ml of 0.25 N NaOH. The intensity of the products of this reaction (p-nitrophenol) was measured at 405 nm (King and Armstrong, 1934). The amount of the p-nitrophenol released by alkaline phosphatase was quantified via the p-nitrophenol standard curve (250 ug/ml). Protein content in the enzyme was estimated as described earlier. The enzyme activity was expressed as (IU/mg protein). The unit can be defined as the quantity of alkaline phosphatase that liberates 1 mg of phosphate glycerol 2-phosphate in 1 hour under standard conditions.

B] Alanine aminotransferase (ALT) [Reitman & Frankel, 1957].

Principle:

The amount of oxaloacetate or pyruvate produced by transamination is reacted with 2,4 dinitrophenyl hydrazine (DNPH) to form a brown-coloured hydrazone, the colour of which in alkaline solution is read at 520 nm.

Reagents Required:

1. ALT substrate-0.532 g alanine and 6.0 mg a-ketoglutaric acid were added to 0.1 ml of IN NaOH prepared in phosphate buffer (0.01M, pH 7.5). Final quantity was adjusted to 20 ml with phosphate buffer (pH 7.5).

2. DNPH reagent-10 mg of dinitrophenyl hydrazine was added to 4.25 ml conc. HCI and the final quantity was adjusted to 20 ml with distilled water.

Protocol:

To this 0.1 ml of serum or 5% liver tissue homogenate (in 0.01M phosphate buffer, pH 7.0) was added to assay the enzyme activity. A suitable enzyme blank was also prepared by taking 0.5ml of substrate and 0.1 ml of distilled water. They were incubated further for another 15 minutes. The reaction was stopped by the addition of 0.5 ml dinitrophenylhydrazine reagent. They were mixed thoroughly and kept at room temperature (25°C) for 20 minutes. 5 ml of 0.4 N NaOH was added to develop the colour, intensity of which was read against the enzyme blank at 540 nm . The product formed (pyruvate) during this reaction time was quantified with the help of a standard curve of pyruvate (220 µg/ml). The enzyme activity was expressed as ug of pyruvate formed/min reaction/ mg of enzyme protein. Protein content in the enzyme was estimated as described earlier.

3.12 Genotoxicity

A] Comet assay [Singh et al., 1988].

Principle:

The principle of the comet assay is based on the migration of negatively charged, fragmented DNA strands when subjected to an electric field, facilitated by the presence of strand breaks. Briefly, a single cell suspension (following exposure to a physical or chemical agent, as relevant) in low melting point agarose is layered onto glass microscope slides and lysed in a high salt solution to generate nucleoid bodies. In the alkaline variant of the comet assay (alkaline comet assay, ACA), the DNA relaxes and unwinds, and is electrophoresed under alkali conditions, neutralized, stained with a fluorescent dye, and finally, visualized and analyzed under a microscope.

Reagents Required:

1. 0.5% Low Melting Agarose: 0.25 g of Low Melting Agarose was dissolved in 50ml of 1X PBS.
2. 1% Normal Melting Agarose: 0.50 g of Normal Melting Agarose was dissolved in 50ml of 1X PBS.
3. 1X Phosphate Buffered Saline (pH=7.4): 8.0 g of Sodium Chloride (NaCl) , 0.20 g of Potassium Chloride (KCl), 1.40 g Na2HPO4 and 0.27 g of KH2PO4 were dissolved in 100 ml distilled water after adjusting the pH using Sodium Hydroxide flakes. This stock solution of 10X PBS was diluted to 1X PBS and used.
4. Lysis buffer (pH 10): 14.6 g of Sodium Chloride (2.5M NaCl), 3.74 g of Disodium salt of EDTA (100mM $C_{10}H_{14}N_2O_8.2Na2H_2O$), 0.12 g of Tris HCl was mixed in 100ml distilled water. 89 ml of this stock solution was mixed in 0.1 ml of 1% Triton X and 10 ml of 10% DMSO (dimethyl sulfoxide) was added after adjusting the pH to using Sodium Hydroxide flakes.
5. 1% Triton X: 1 ml of Triton X(10mM) liquid was diluted to 100ml using distilled water.

6. 10% DMSO: 10 ml of DMSO was diluted to 100ml using distilled water.

7. Neutralisation buffer (pH 7.5): 4.84g of Tris Base (400mM) was added in 100 ml distilled water after adjusting the pH to 7.5. It was stored at room temperature and chilled right before use.

8. Unwinding/ Electrophoresis buffer: 20.0 g of Sodium Hydroxide (NaOH) was mixed in 50 ml in an exothermic reaction. Likewise, 1.49 g of Disodium salt of EDTA ($C_{10}H_{14}N_2O_8.2Na.2H_2O$) was mixed in 20 ml distilled water after adjusting the pH to 10.

To prepare the working solution, 27 ml of NaOH, 4.5ml Disodium salt of EDTA ($C_{10}H_{14}N_2O_8.2Na2H_2O$) and 1.8 ml of DMSO was diluted to 1000 ml distilled water.

9. Ethidium Bromide solution: 0.01 g of Ethidium Bromide was added in 50 ml distilled water and stored in Amber Bottles. From this stock solution, 100 µl was diluted to 1 ml distilled water to prepare the working solution in an Eppendorf tube, covered with aluminum foil. Due care was ensured while handling ethidium bromide with the use of gloves.

Protocol:

The alkaline comet assay was performed as per Singh et al. (1988) with slight modifications. Care was taken to prevent additional DNA damage resulting from direct exposure to visible light by performing all steps in the dark at 4°C. Fully frosted microscope slides (Fisher Scientific, Cat no.: 12-544-5CY, USA) were coated with a thin layer of 1% normal melting- point agarose and allowed it to solidify. Subsequently, 20 µL of bone manow suspension (in PBS) was mixed with 80 µL of 0.5% low melting agarose, pipetted onto the pre-coated slides and covered with a cover slip the agarose layer on the slide was chilled for 5 min and after its solidification, the cover slip was removed A final layer of 0.5% low melting agarose was placed over the second layer and allowed to solidify.

Slides with bone marrow cells embedded in agarose were submersed in a cold, alkaline (4°C, pH 10) lysis solution [2.5 M NaCl, 100 mM Na_2EDTA, 10 mM This base (pH 10), 1% Triton X-100, 10% DMSO] and maintained for 4 h. They were then placed in an alkaline electrophoresis buffer of pH 13 (1 mM Na_2EDTA/300 mM NaOH) for 25 min to induce unwinding of DNA strands. The slides were then transferred to an electrophoresis tank with fresh alkaline electrophoresis buffer and electrophoresis was performed at field strength of 20V/125 mA for 25 min at 4°C. The DNA in the agarose was neutralised by incubation in 0.4 M Tris (pH 7.4) at room temperature (26°C) for 5 min DNA was stained by placing 20 µL/mL of ethidium bromide on the agarose, covered with a cover slip and incubated for 5 min in dark The DNA damage was quantified by observing the cells under 20X objective of a fluorescence microscope Olympus BX 53, Japan) equipped with an excitation filter of 510-560 nm and an emission filter of 590 nm One hundred comet images were recorded for each sample (2 slides, 50 images from each slide). The comets were analyzed by the image analysis software CASP.

3.13 Statistical Analysis

Statistical analyses were done using GraphPad Prism 10.2.2 software. The results were expressed as mean ± SD (Standard Deviation). One-way ANOVA (analysis of variance) and Pearson's Correlations was carried out to compare the differences of means among multi-group data calculating p, F and r values. The statistical software system was also used to perform a post hoc multiple comparison test (Dunnett's test) after ANOVA. A level of $p<0.05$ was considered to be significant, $p \leq 0.01$ as highly significant and $p<0.001$ as extremely significant

4. Results

4.1 General Examination.

MnO_2-NPs treated mice with high dose, showed dullness, irritation and moribund symptoms. However, no morphological changes were observed in both the groups.

4.2 Comet Assay.

The results of comet assay after a 14-day repeated oral treatment with 100 and 500 mg kg–1 b.w per day of MnO_2-NPs in male Swiss Albino Mice are shown in (Fig. 14). An increase in the % tail DNA was observed after a 14-day repeated oral dose of 500 mg/kg b.w MnO_2-NPs, but these results were not statistically significant at all time intervals compared with the control group ($p > 0.05$).

4.3 Histopathological Examinations.

Mice exposed to 100 mg/kg b.w of MnO_2 NPs showed somewhat normal architecture of the liver and kidney tissues, except for some mild sinusoidal dilation and congestion of portal vein in the liver, and few distorted glomeruli in the kidney tissue. However, those treated with the high dose showed inflammation of inflammatory cells near the portal vein, binucleated hepatocytes, sinusoidal dilation, congestion and dilatation of portal vein in the liver tissue, while inflammatory cell infiltration and many distorted glomeruli were observed in the kidneys.

4.4 Effect of MnO_2-NPs on the Biomolecules in the liver and kidney tissue.

The liver and kidney tissues of mice were utilized to assess the impacts of orally administered MnO_2-NPs at two different doses (i.e., 100 and 500 mg/kg b.w.). Various biochemical

parameters and enzymes, including total proteins, carbohydrates, free sugars, albumins, GSH, TBARS, urea, creatinine, ALT, ALP, SOD, and CAT, were hence analyzed. Figures 1 to 13 illustrate the changes observed in biomolecule and enzyme concentrations in mice exposed to the test substance.

The administration of MnO_2-NPs resulted in a slight decrease in the protein content of Experimental 2 group, as illustrated in (Fig 3). However, this decrease was not statistically significant, compared to both the control and exp 1 group. On the other hand, MnO_2- NPs exposure increased the carbohydrate concentration in the 2 exposure groups. According to ANOVA this increase was found to be insignificant (Fig 1).

The Free sugar concentration was significantly increased in both the experimental groups when compared to the control, but this increase was not dose-dependent ($F = 149.6$, $p < 0.0001$) (Fig 2). Similarly, a significant increase was also observed in the concentration of albumin in both the experimental groups when it was compared with the control ($F = 38.15$, $p < 0.0001$) (Fig 4). Treatment with MnO_2-NPs showed a significant dose-dependent increase in the levels of bilirubin in exposure 2 group, while the increase in exposure 1 group was found to be insignificant compared to the control. ANOVA analysis revealed significant differences with regard to levels of bilirubin across the exposure sets (F value= 4.874, $p = 0.0282$) (Fig 5).

The daily oral administration of MnO_2-NPs to mice for 14 days resulted in a significant elevation in creatinine levels in exp group 2 ($F= 6.17$, $p = 0.0144$) (Fig 12), whereas exp group 1 showed a non-significant increase compared to the control. In contrast, the levels of urea exhibited a non-significant decrease in exp group 1, while both the control and exp l group 2 seemed to be relatively unaffected after the treatment (Fig 13).

4.4 Effect of MnO_2-NPs on the Liver Enzymes.

The levels of ALT showed a significant and a dose-dependent increase in both the exp groups as compared to the control. ANOVA analysis revealed significant differences with regard to levels of ALT across the exposure sets ($F = 23.22$, $p < 0.0001$) (Fig 10). On the other hand, there was a slight, albeit statistically insignificant rise in the levels of ALP in both the exp groups when compared to the control (Fig. 11).

4.5 Effect of MnO_2-NPs on Antioxidants.

The results of Catalase estimation illustrated in (Fig 8) shows elevated levels of the enzyme in both the test groups as compared to the control However, ANOVA analysis revealed no significant differences in catalase levels among the exposure sets. Likewise, the concentration of Malondialdehyde (MDA) depicted in (Fig 6), exhibited an increase in its concentration in both the Experimental Groups. However, according to ANOVA, these differences were found to be insignificant.

Following exposure to MnO_2-NPs, a slight, non-significant rise in reduced glutathione levels was noted across all exposure sets when compared to the control (Fig 7). A Significant increase was observed in the levels of Superoxide Dismutase (SOD) in the exp group 2 ($F = 14.05$, $p=0.0007$) while a minor, non-significant increase was seen in exp group 1 compared to the control. ANOVA analysis revealed significant differences with regard to levels of SOD across the exposure sets ($F = 14.05$, $p = 0.0007$) (Figure 9).

4.6 Pearson’s Correlation analysis (Table 2)

According to Pearson's correlation test, protein concentration showed a strong significant negative correlation with respect to the levels of SOD ($p = 0.013$, $r = -0.622$) in the liver tissue while the levels of SOD were significantly and positively correlated to levels of bilirubin ($p = 0.023$, $r = 0.581$), ALT ($p = 0.020$, $r = 0.591$) and ALP ($p = 0.003$, $r = 0.719$). A significant positive association was observed between the increase in the levels of bilirubin and the increase in the levels of TBARS ($p = 0.042$, $r = 0.530$) and ALT ($p = 0.008$, $r = 0.659$).

While correlation analysis revealed a statistically significant positive relationship between free sugars concentration and the levels of albumins ($p = 0.006$, $r = 0.67$), bilirubin ($p = 0.015$, $r = 0.62$) and the levels of ALT ($p = 0.005$, $r = 0.70$).

1) EFFECT OF MnO_2-NPs ON VARIOUS BIOMOLECULES IN THE LIVER.

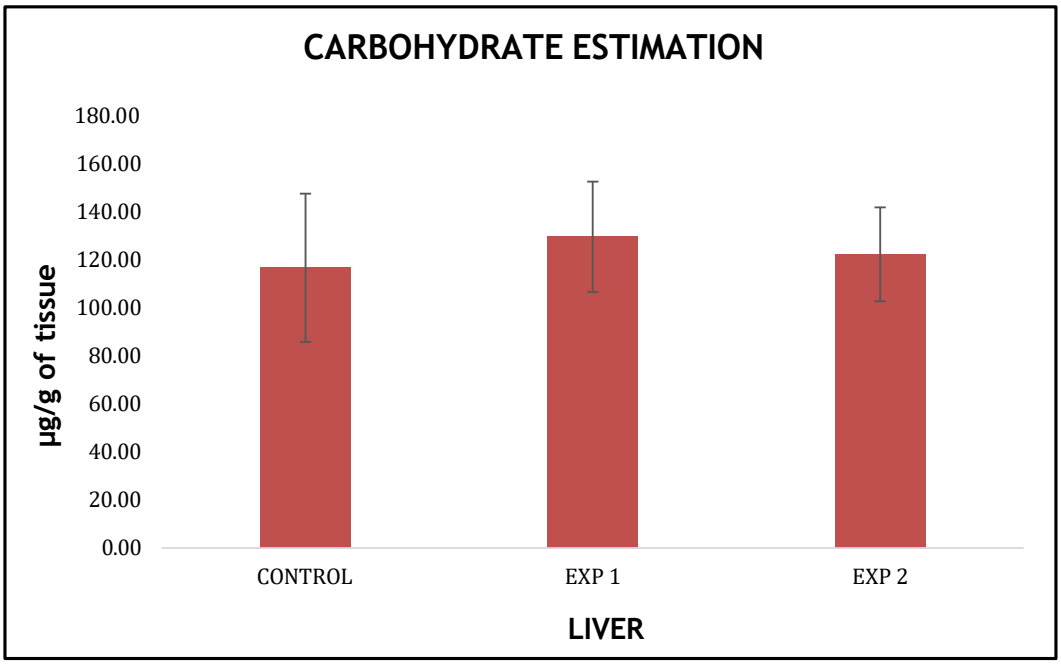

Figure 1. Effect of MnO_2-NPs on Carbohydrate content in the liver of mice.

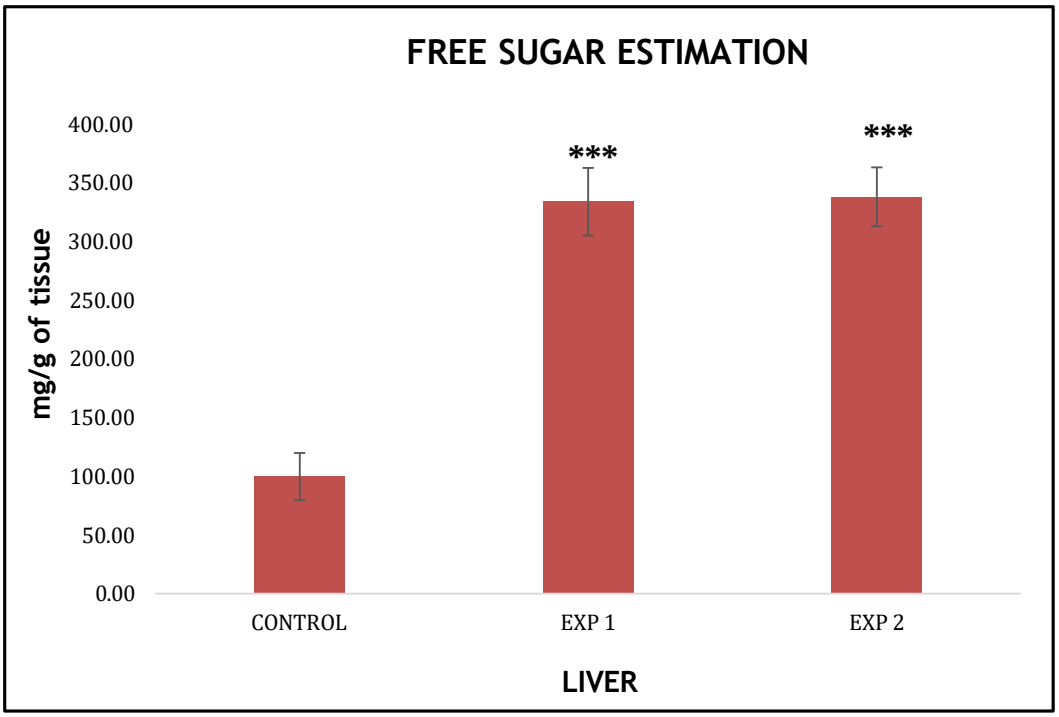

Figure 2. Effect of MnO_2-NPs on Free Sugar content in the liver of mice. ($p<0.001$***); ($p<0.0001$****)

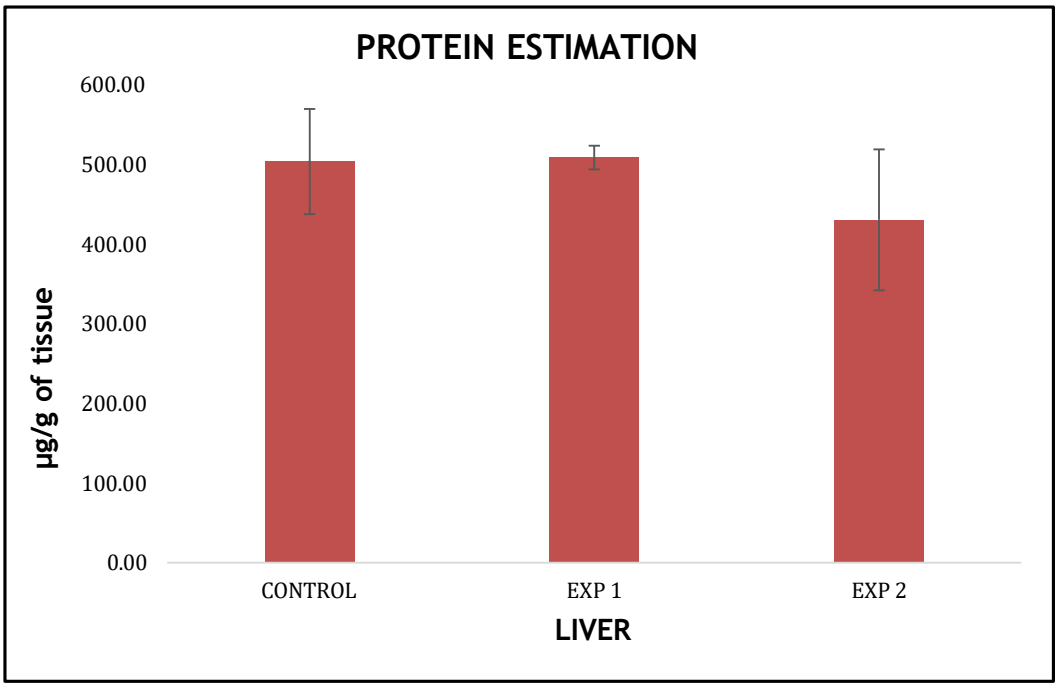

Figure 3. Effect of MnO_2-NPs on total protein content in the liver of mice

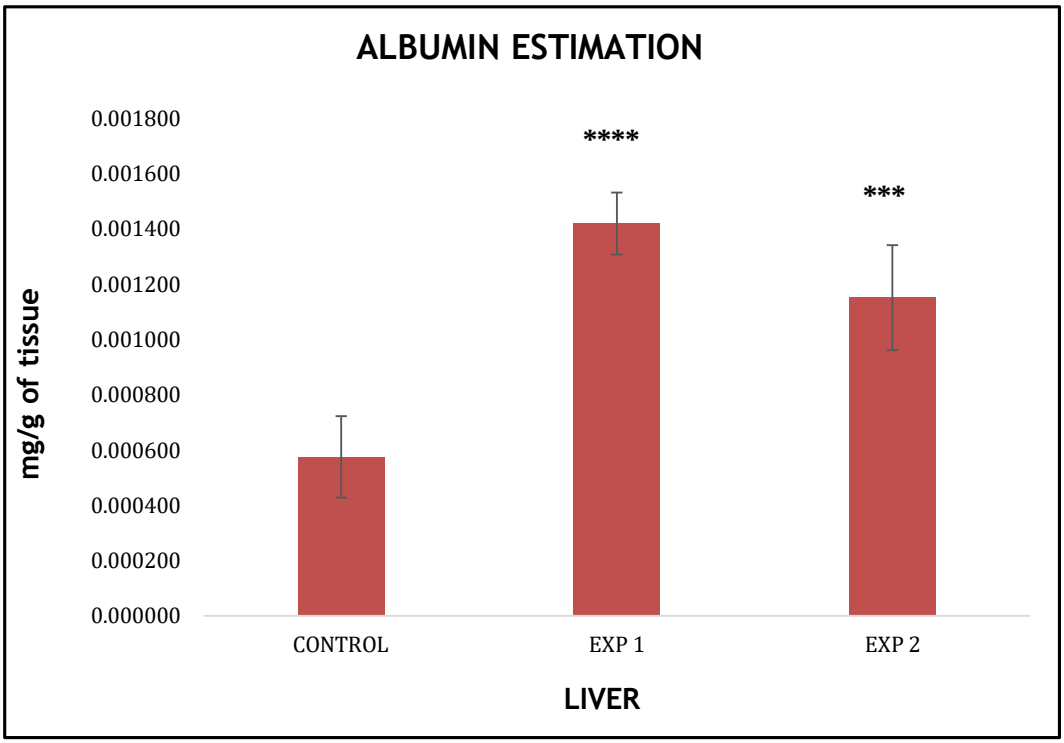

Figure 4. Effect of MnO_2-NPs on Albumin content in the liver of mice. ($p<0.001$***); ($p<0.0001$****).

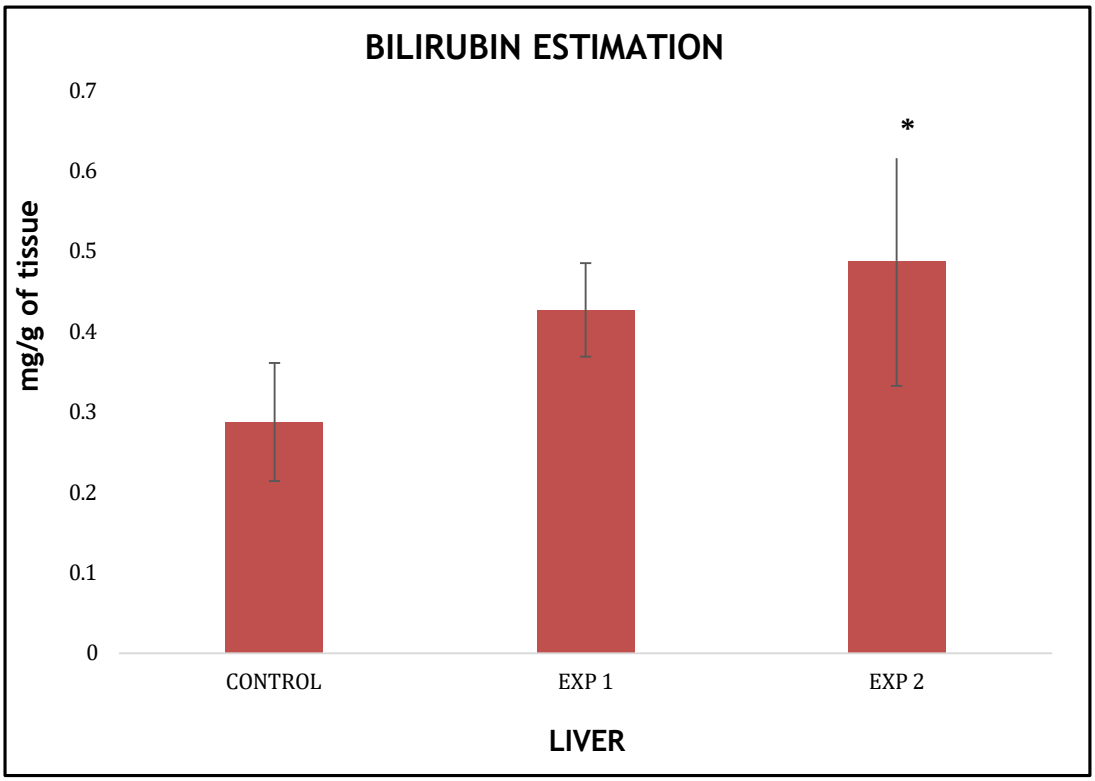

Figure 5. Effect of MnO_2-NPs on Bilirubin levels in the liver of mice. ($p<0.05$*)

2) EFFECT OF MnO_2-NPs ON THE ANTIOXIDANT LEVELS IN LIVER

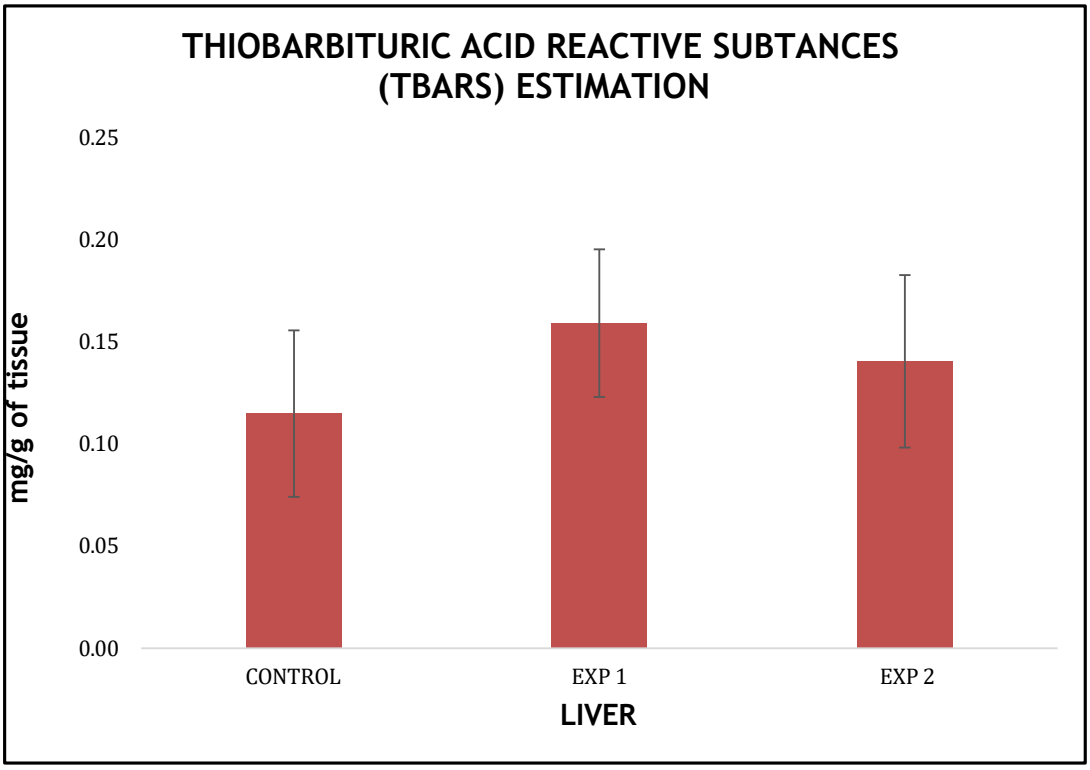

Figure 6. Effect of MnO_2-NPs on Thiobarbituric Acid Reactive Substances (TBARS) content in the liver of mice.

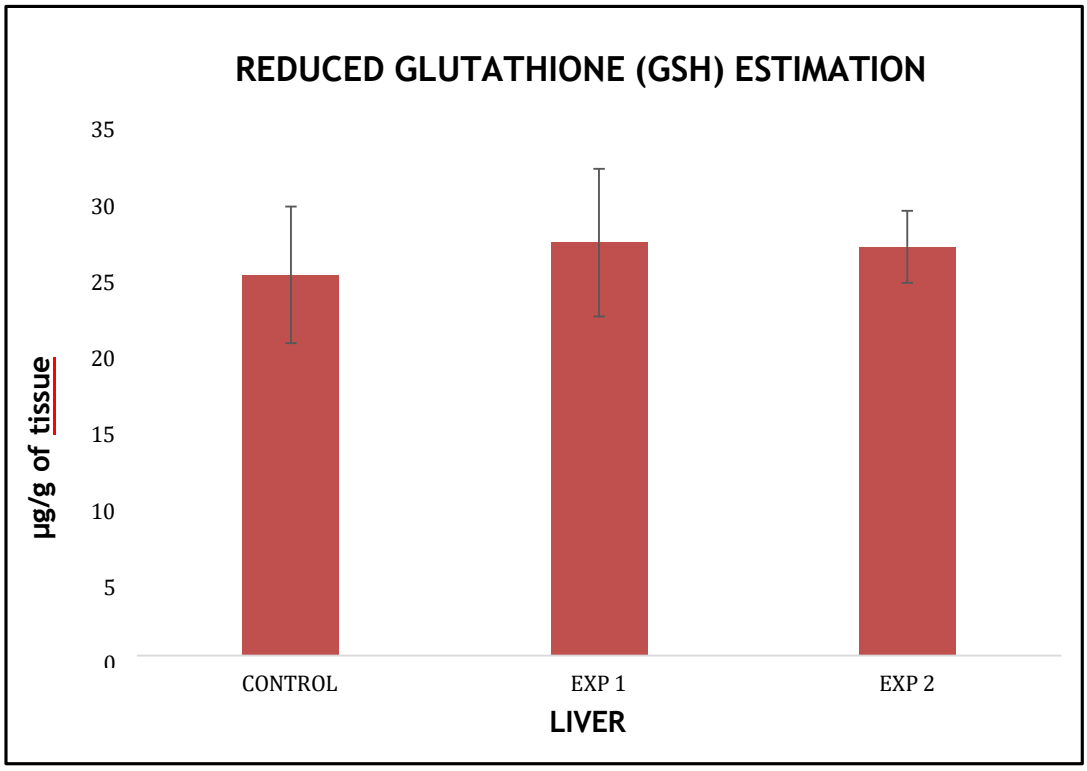

Figure 7. Effect of MnO_2-NPs on Reduced Glutathione content in the liver of mice.

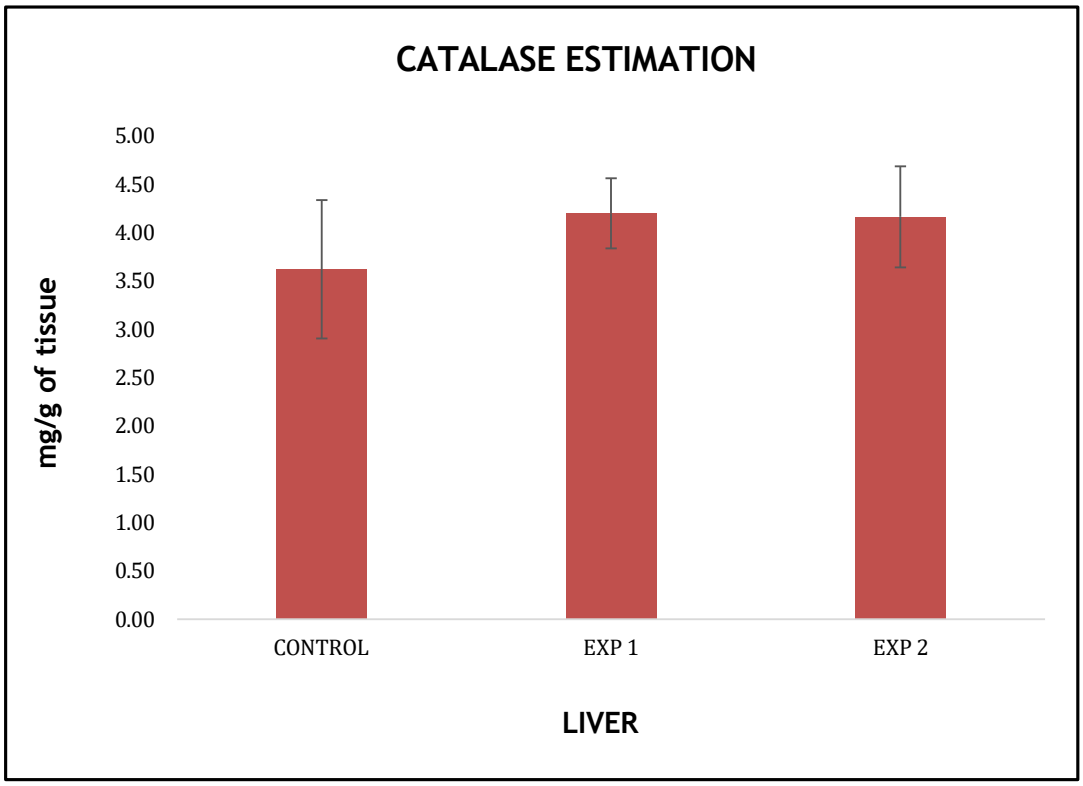

Figure 8. Effect of MnO_2-NPs on Catalase activity in the liver of mice.

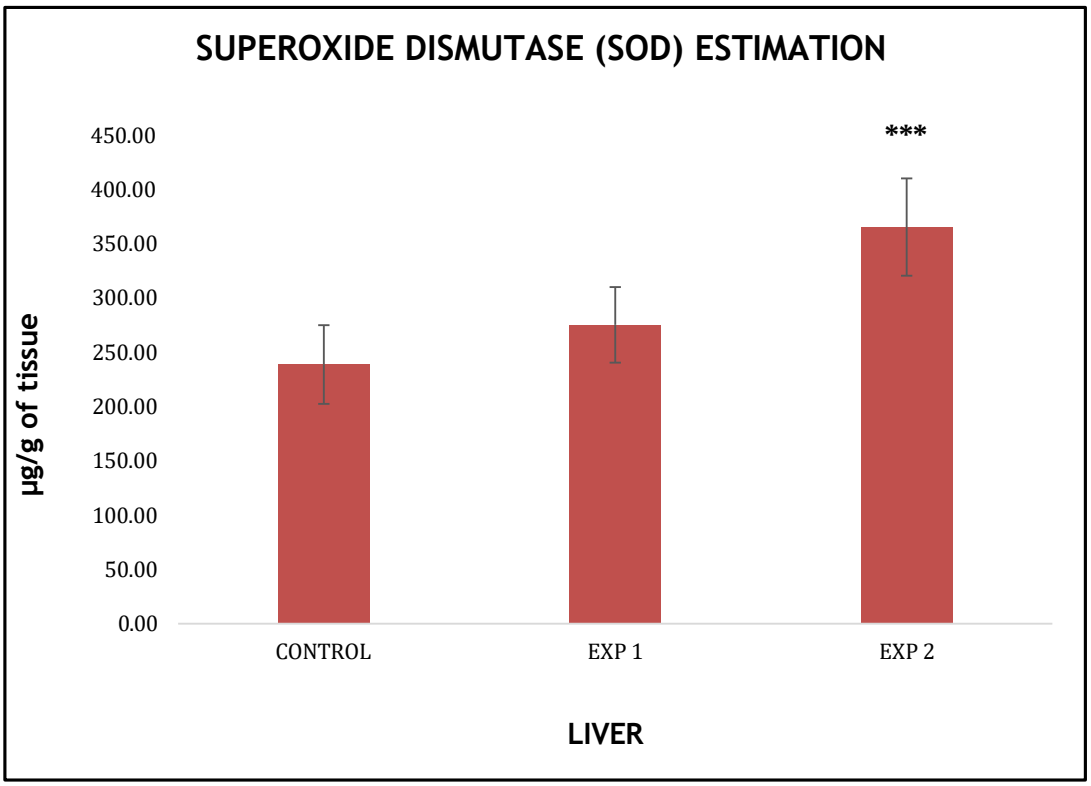

Figure 9. Effect of MnO_2-NPs on Superoxide Dismutase (SOD) activity in the liver of mice. ($p<0.001$***).

3) EFFECT OF MnO_2-NPs ON THE LIVER ENZYMES

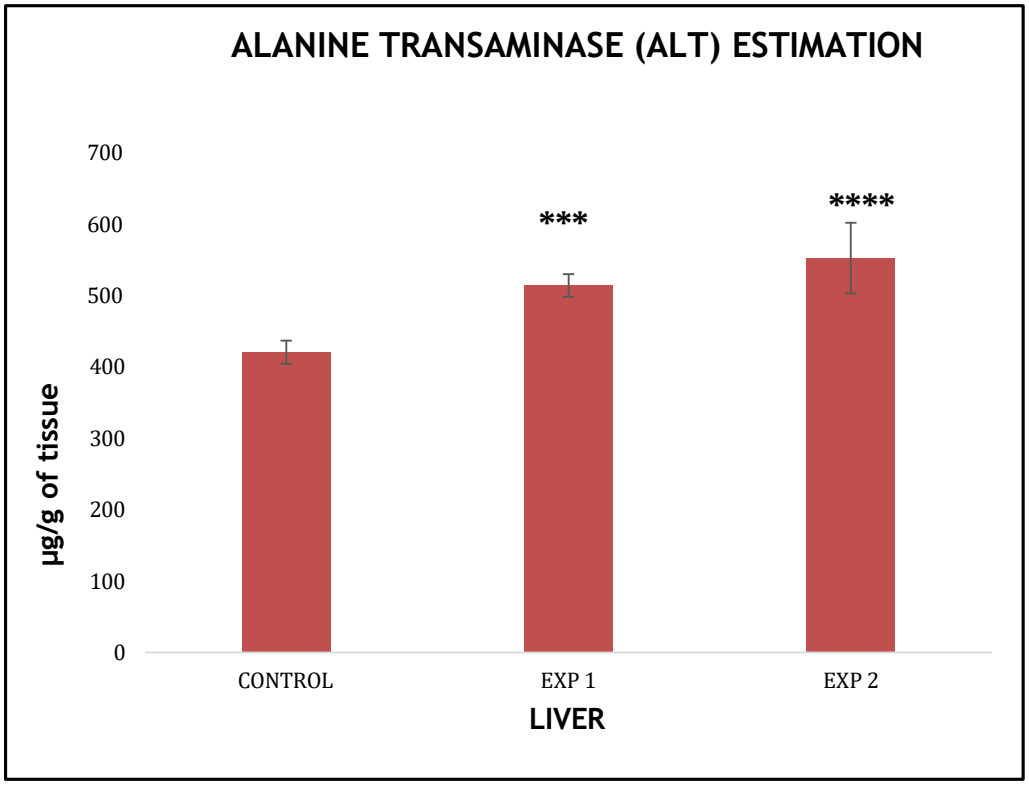

Figure 10. Effect of MnO_2-NPs on Alanine Aminotransferase (ALT) activity in the liver of mice. ($p<0.001$***); ($p<0.0001$****).

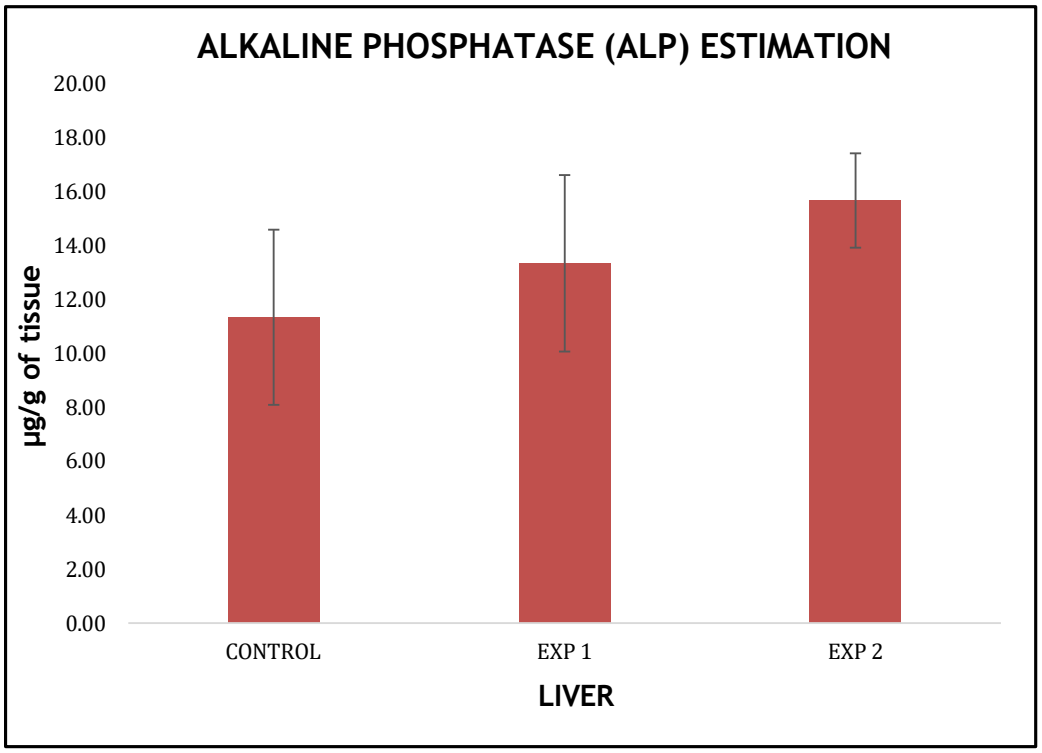

Figure 11. Effect of MnO_2-NPs on Alkaline Phosphatase activity (ALP) in the liver of mice.

4) EFFECT OF MnO_2-NPs ON BIOMOLECULES IN THE KIDNEY

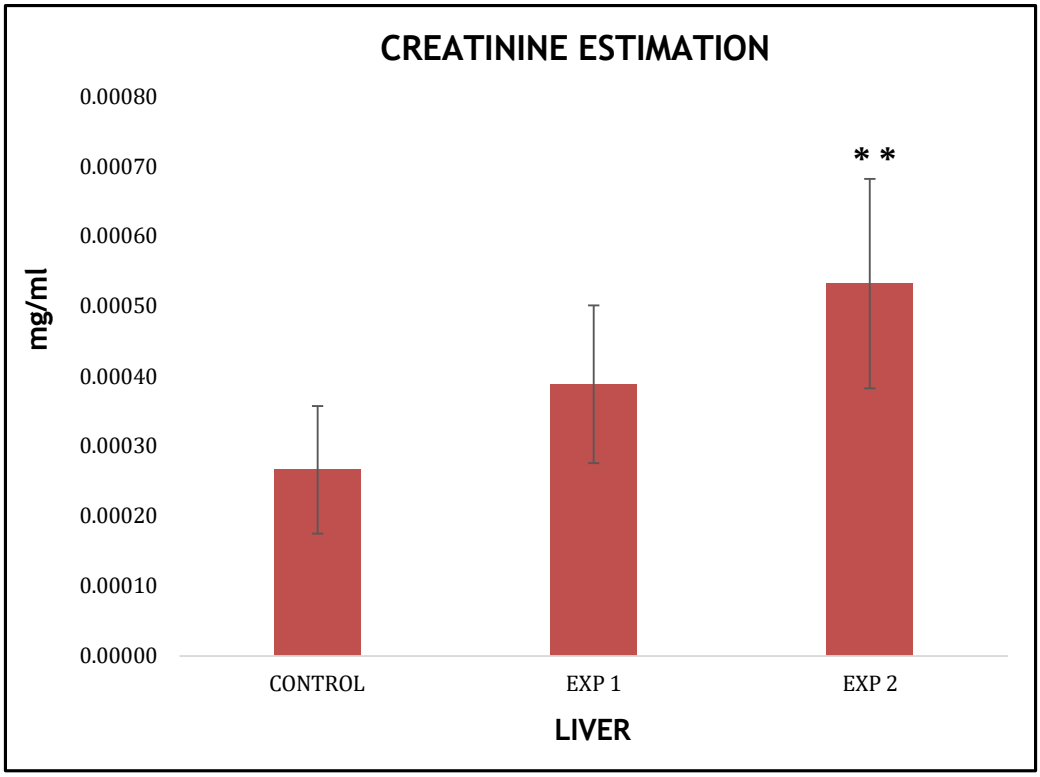

Figure 12. Effect of MnO_2-NPs on Creatinine content in the kidney of mice. ($p<0.01$**).

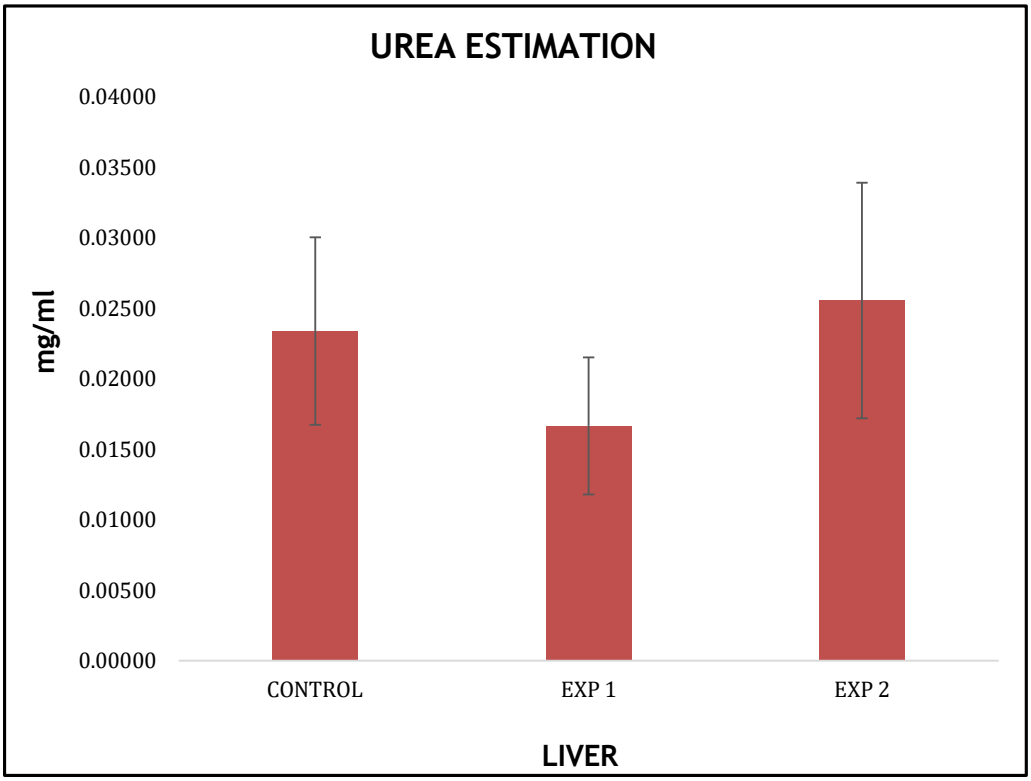

Figure 13. Effect of MnO_2-NPs on Urea content in the kidney of mice.

GENOTOXICITY OF MnO_2-NPs

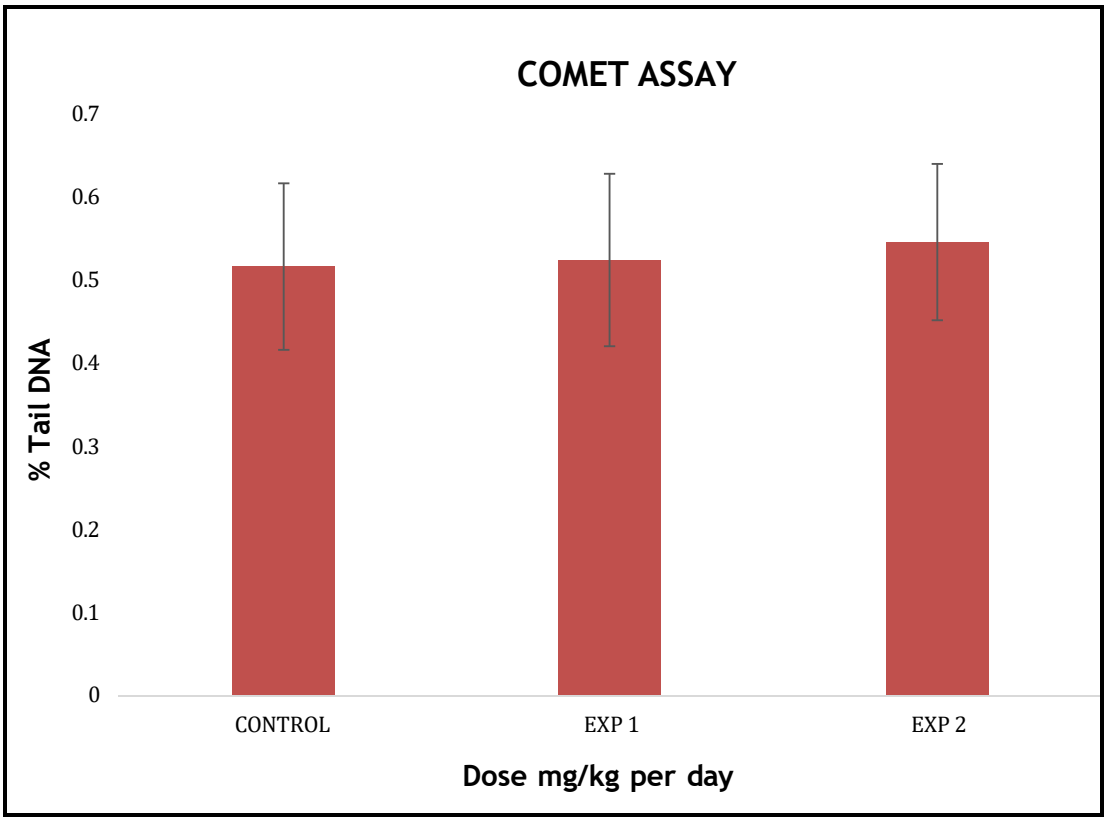

Figure 14. Mean % tail DNA in bone marrow cells of mice after 14 days of repeated exposure to 2 different doses (low dose: 100 mg/kg b.w & High dose: 500mg/kg b.w)

6) HISTOPATHOLOGICAL EXAMINATION OF LIVER

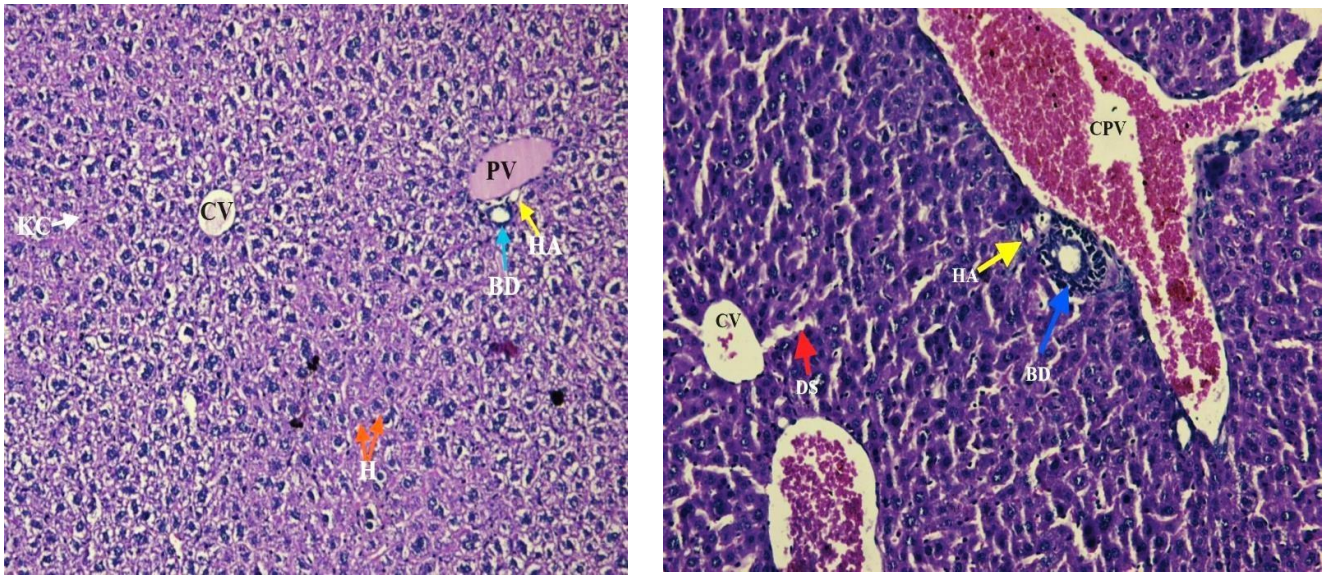

Figure 15a) Hematoxylin and eosin stained Liver sections of adult mice: A] Control Group, B] Experimental 1 group showing (YELLOW ARROW) HA= Hepatic Artery, (BLUE ARROW) BD= Bile Duct, (RED ARROW) DS=Dilated Sinusoid in Exp 1 and Hepatocytes in Control, CV= Central Vein, CPV= Congestion And Dilation in Portal Vein, PV = Portal Vein.

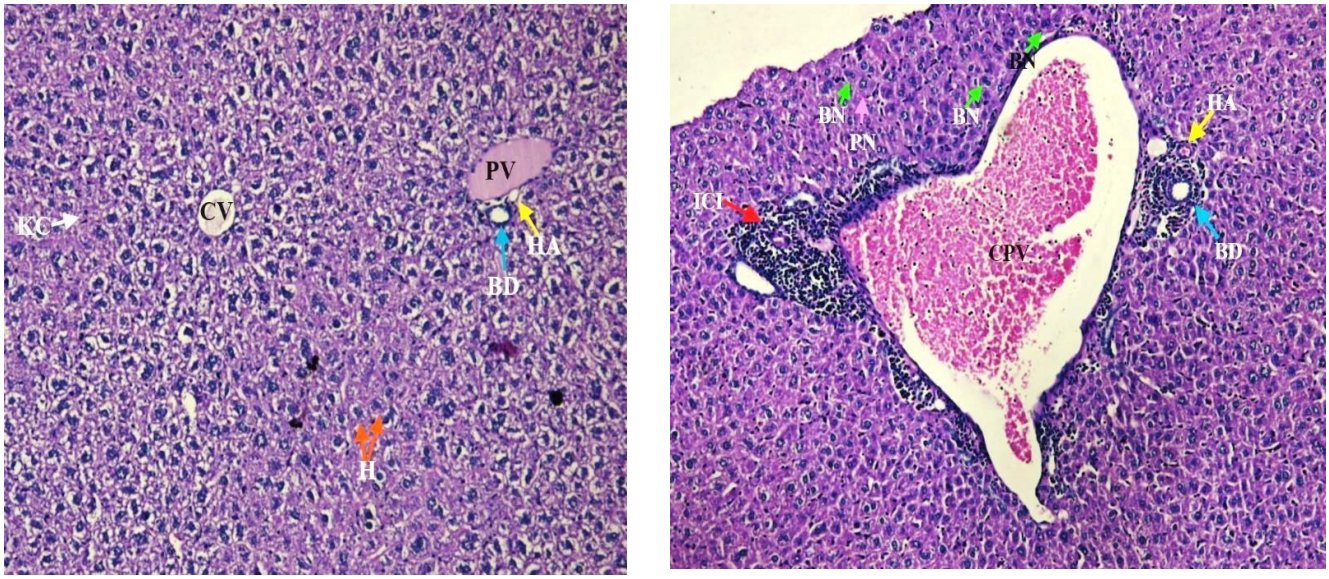

Figure 15b). Hematoxylin and eosin stained Liver sections of adult mice: A] Control group and B] Exp 1 group showing (YELLOW ARROW) HA= Hepatic Artery, (BLUE ARROW) BD= Bile Duct, (WHITE ARROW) CV= Central Vein, (RED ARROW) H= Hepatocytes in control and ICI= Iflammatory Cell Infiltration in Exp 2 group, CPV= Congestion And Dilation in the Portal Vein, PV= Portal Vein, BN= Binucleated hepatocytes, PN= Prominent Nucleus of hepatocyte.

7) HISTOPATHOLOGICAL EXAMINATION OF KIDNEYS

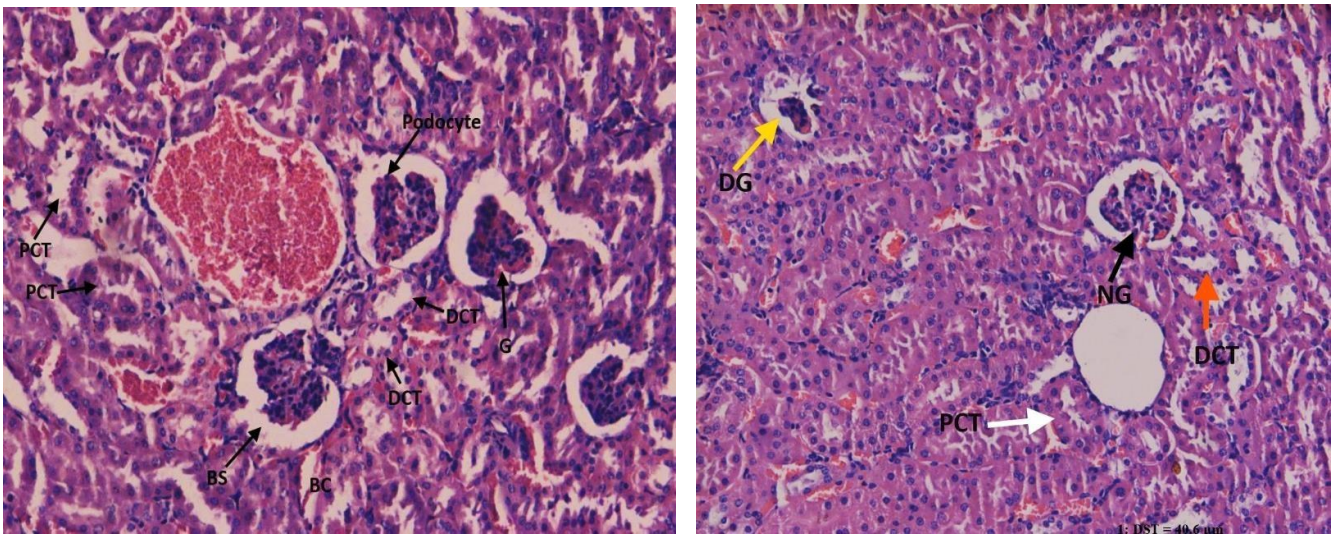

Figure 16a) Hematoxylin and eosin stained kidney sections of adult mice: A] Control B] Experimental 1 group, showing G=Glomerulus, BS= Bowman's Space, BC= Bowman's Capsule, (WHITE ARROW) PCT= Proximal Convoluted Tubule, (RED ARRROW) DCT=Distal Convoluted Tubule, (YELLOW ARROW) DG= Distorted Glomerulus with wide Bowman's Space, Podocytes.

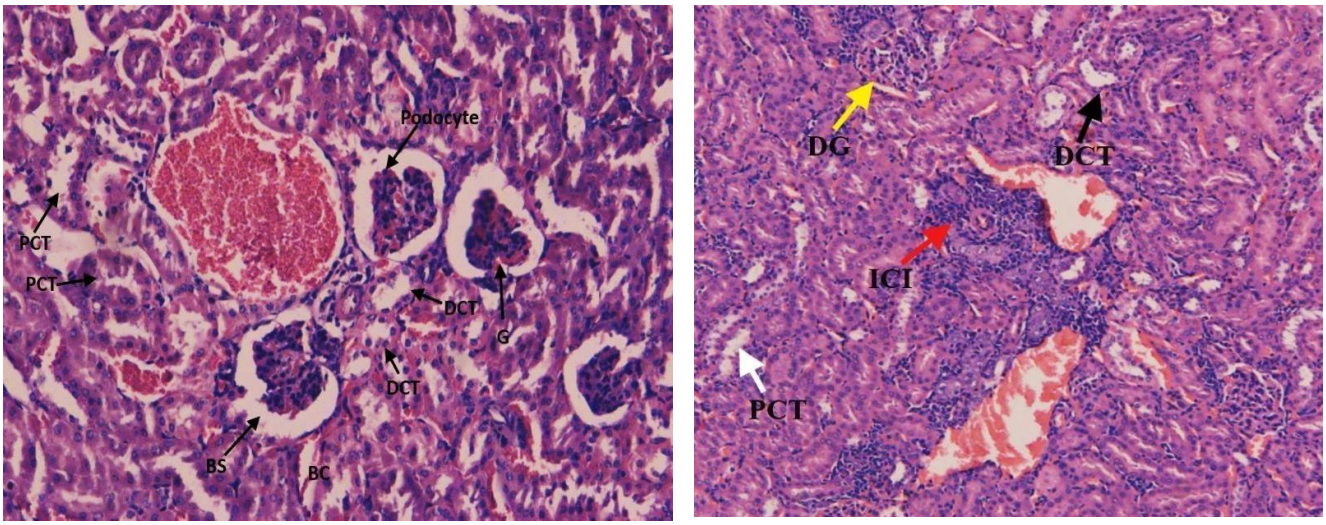

Figure 16b) Hematoxylin and eosin stained kidney sections of adult mice: A] Control, B] Experimental 2 group showing (YELLOW ARROW) DG= Distorted Glomerulus with narrow Bowman's Space, (RED ARROWW) ICI= Inflammatory Cell Infiltration, (WHITE ARROW) PCT= Proximal convoluted, (BLACK ARROW) DCT= Distal Convoluted Tubule and podocytes.

Table 2: PEARSON'S CORRELATION BETWEEN DIFFERENT BIOMOLECULES AND ENZYMES

PEARSON r VALUE	PROTEINS	ALBUMINS	FREE SUGARS	BILIRUBIN	TBARS	SOD	ALT
PROTEINS	–						
ALBUMINS	0.004	–					
FREE SUGARS	-0.204	**0.829*** **	–				
BILIRUBIN	-0.166	0.346	**0.623***	–			
TBARS	0.316	0.441	0.404	**0.530***	–		
SOD	– **0.622****	0.275	0.491	**0.581***	0.294	–	
ALT	-0.215	**0.643***	**0.7****	**0.659****	0.302	**0.590***	–
ALP	-0.432	0.340	0.488	0.353	0.453	**0.718****	0.444

5. DISCUSSION

In the coming years, nanotechnology is set to become a crucial component of the global economy and daily life. However, there is a growing concern about the risks associated with human and environmental exposure to nanoparticles (NPs) due to their small size and large surface area, enabling them to enter the human body through various pathways, raising worries about their potential toxic effects, whether intentional or accidental (Singh et al., 2013).

The oral route is commonly employed to assess NP toxicity, given the likelihood of NPs being ingested more frequently compared to exposure through the skin or inhalation (Rashidi & Khosravi-Darani, 2011). This study aimed to assess the biochemical, genotoxic and histopathological effects of MnO_2-NPs in the liver and kidney tissues of Swiss Albino mice after 14 days of repeated oral treatment. The results of the present study revealed that the oral administration of 100 and 500 mg/kg b.w of MnO_2-NPs in Swiss Albino Mice did not cause any obvious adverse effects in a 14-day acute toxicity study.

Biochemical enzymes and their levels serve as initial diagnostic tools for assessing changes caused by xenobiotics. Acute manganese (Mn) toxicity, primarily affects the liver due to its crucial role in xenobiotic processing, leading to alterations in enzyme composition from nanoparticle deposition (Kim et al., 2009). Consequently, hepatocytes are the primary target of nanoparticles post-oral ingestion, given their involvement in detoxification. Moreover, the high penetration capability of the metal oxide nanoparticles enhances their interaction with the hepatocytes (Elder et al., 2006). The elevated serum protein and enzyme levels serve as reliable indicators of hepatocellular damage, inflammation, kidney dysfunction, and cholestasis (Wquimby & Hluong, 2007). Kidney tissue has been recognized as a potential site of nanoparticle toxicity following the liver (Teodoro et al., 2016). The kidneys are recognized for eliminating harmful substances from the bloodstream, so nanoparticles entering the circulatory

system are later filtered by the renal system (Schipper et al., 2009; Gao et al., 2012).

Glucose serves as a universal energy source in all living organisms. Any changes in glucose levels can disrupt various physiological processes (Canli et al., 2017). The present investigation demonstrated that oral exposure to MnO_2 nanoparticles led to a significant increase in free sugar levels in both test groups. Additionally, the high dose group exhibited a significant increase in glucose levels compared to the low dose group, however this rise was found to be insignificant when compared to the control group. Our results are consistent with previous studies reported by Mousavi et al. (2016) and Alarifi et al. (2017), who observed similar alterations in animal biochemical profiles following sub-chronic exposure to nanosized MnO_2 particles. Elevated glucose levels activate several pathogenic pathways, including the generation of reactive oxygen species (ROS). MnO_2's ability to restore imbalances in antioxidants and liver enzymes, responsible for cellular dysfunction and destruction, may have contributed to hyperglycemia in our test groups.

Albumins, the predominant proteins in blood plasma, play a crucial role in transporting a wide range of endogenous and exogenous substances, such as fatty acids, amino acids, steroids, and various drugs (Baral et al., 2017). Although there were no significant changes in total protein levels, male mice treated orally with MnO_2-Nps showed increased levels of albumin. However, this increase was not dose-dependent and thus was not considered a toxic response. These results align closely with those reported by Sun et al. (2021). Albumin is also the most abundant circulating antioxidant that helps to prevent oxidative damage. During the process of combating oxidative stress induced by metals, albumin concentration may initially increase and then subsequently decrease. This explains the observed increase in albumin concentration in both experimental groups compared to that of the control (Dobrakowski et al., 2014; Baraka-

Vidot et al., 2013). Hyperalbuminemia has also been documented in rats exposed to Mn (Chtourou et al., 2013). Bilirubin serves as an early indicator of toxicity caused by NMs. $Mn0_2$-NPs caused a substantial increase in the levels of bilirubin, in Experimental 2 group when compared to control and Experimental Group 1. Our results are in agreement with Hafez et al., 2018; & Hussain et al., 2006). The elevated levels of bilirubin may be associated with increased hemolysis or hepatic complications either in metabolism or secretion of conjugated products.134.5 or it may be due to the ability of bilirubin to act as an effective scavenger of ROS in the body, thereby providing protection against oxidative damage (Mireles et al., 1999)

Since 1955, Serum aminotransferases such as aspartate aminotransferase (AST) and alanine aminotransferase (ALT) have been used as standard markers for hepatotoxicity (Nalpas et al., 1986). Although AST is distributed across various tissues including the liver, kidneys, heart, and pancreas, approximately 80% of AST resides in the mitochondria of hepatocytes, resulting in its slower release compared to ALT. But since ALT is predominantly localized in hepatocyte cytosol, it inherently becomes a more sensitive indicator of hepatocellular damage than AST. Additionally, within certain limits, ALT can offer a quantitative assessment of liver damage severity (Al-Mamary et al., 2002). Our results showed that MnO2-NPs caused significant alterations in the activity of ALT in the liver of the exposed mice in a dose-dependent manner.

Because ALT does not originate from the extracellular fluid, an elevation in its levels indicates potential cell membrane disruption of liver cells. (Oloyede et al. 2017). Several other nanoparticles have exhibited a similar pattern concerning the concentration of ALT (Park et al., 2010; Singh et al., 2013; Kumari et al., 2012; Chinde & Grover, 2017). Another reason for elevated ALT levels can be attributed to high free sugars levels, as ALT is also known as a gluconeogenic enzyme which can lead to conditions such as type 2 diabetes and insulin

resistance (Qian et al., 2015).

ALP, also known as a cholestatic liver enzyme, is closely linked with cholestasis, a condition marked by either partial or complete blockage of the bile ducts. In cases of inflammation or dysfunction of the bile duct, ALP may accumulate within the liver and subsequently leak into the bloodstream (Popper, 1968). Although a dose-dependent increase in alkaline phosphatase (ALP) levels was observed in the treated mice, these changes however, were not statistically significant when compared to the control group, implying good condition of the bile ductules.

Numerous studies have also focused on the generation of reactive oxygen species (ROS) and oxidative stress induced by various nanoparticles (NPs). ROS production stands out as a key contributor to nanoparticle toxicity, as highlighted in studies by Khan et al. (2012), Sharma et al. (2012), and Manke et al. (2013). Alterations in the oxidative/antioxidative balance, is often marked by an increase in oxidant levels and a decrease in antioxidant components. The antioxidant system consist of enzymatic components like superoxide dismutase (SOD), glutathione peroxidase (GPx), glutathione-S-transferase (GST), and catalase (CAT), along with non-enzymatic elements such as glutathione (GSH) and Thiobarbituric acid Reactive Substances (TBARS). These elements play vital roles in neutralizing the oxidants and combating oxidative stress induced by toxic substances (Pena-Llopis et al., 2001).

Given the liver's role as the primary site for nanoparticle accumulation (Yang et al. 2008), various oxidative stress parameters were investigated in liver homogenates of mice treated with MN02-NPs. Our results revealed a non-significant increase in MDA, CAT, and GSH levels in NP-treated mice, hinting at the possible induction of free radical generation by the nanoparticles. SOD, another antioxidant enzyme, is considered as the first line of defense against oxygen-related damage, as it counteracts the harmful effects of free radicals (Lobo et

al., 2010). This study showed that superoxide dismutase levels were significantly increased in the high dose group than the low dose and the control group. This adaptive response likely served to mitigate the adverse effects of nanoparticles by neutralizing free radicals and ameliorating oxidative stress within the body. Notably, during periods of oxidative stress, cells typically boost the expression of key antioxidant enzymes like glutathione peroxidase (GSH-Px), superoxide dismutase (SOD), and catalase (CAT) (Valavanidis et al., 2006; Yildirim et al., 2018). Moreover, various studies have suggested a negative correlation between ROS elevation and the success of the antioxidant system following NP administration in mammals (Yu et al., 2014; Hu et al., 2015; Lei et al., 2015). However, differences in the intervention routes, exposure durations, doses, sample origins, and nanoparticle sizes of MnO2-NPs, have yielded diverse conclusions (Liang et al., 2009).

The levels of urea and creatinine are tested as a measure of kidney function (Wang et al., 2007). Repeated oral exposure to MnO_2 nanoparticles resulted in significant elevation in the levels of creatinine only at the highest exposure dose and a non-significant increase in the low dose group when compared to the control groups, suggesting impaired glomerular filtration in the form of distorted Glomerulus which leads to a decreased surface area for filtration and subsequently reducing the clearance of creatinine. Our findings are consistent with those of (Iavicoli et al. (2016) Wen et al. (2017); Alomari et al. (2020). However, there were no significant differences in urea content among the experimental groups and the control group. Similar results were reported by Jafarzadeh Samanai et al. (2016).

The activity of SOD showed an inverse correlation with the levels of proteins, possibly because oxidative damage to DNA and proteins, resulted into increased protein inactivation or degradation, or reduced gene expression caused by elevated ROS levels. It has been demonstrated that excessive ROS production can inhibit SOD activity, creating a feedback loop

that leads to further ROS accumulation. ROS can induce structural changes in proteins, causing spontaneous fragmentation or increased susceptibility to proteolysis (Davies et al., 1987; Yunoki et al., 1998). Studies have demonstrated that protein carbonyl derivatives, formed during metal-catalysed oxidation and accumulated during ageing, serve as substrates for intracellular proteolytic systems and proteases (Stefanescu et al., 2009). Our findings are similar to (Kim & Lee, 1997; Ramanathan et al., 2002). Elevated levels of SOD were noticed alongside increased bilirubin, ALT, and ALP levels, likely due to oxidative stress causing damage to lipids and cell membranes. This damage can prompt cell apoptosis or death, leading to higher liver enzyme levels like ALP and ALT, as well as bilirubin. Consequently, during oxidative stress, cells usually increase the production of antioxidant enzymes to counteract the excessive generation of free radicals, initiating a self-protective response. Our results are consistent with previous studies (Wang et al., 2009; Hussain et al., 2020).

Elevated liver enzymes are linked with increased oxidative stress, as shown by increased TBARS levels, leading to liver cell damage. Bilirubin acts as an effective scavenger of ROS in the body, providing protection against oxidative damage, hence explaining the rise in bilirubin levels.. However, there's a limit to the protective effects of bilirubin. Our results align with previous studies (Mireles et al., 1999; Annabi Berrahal et al., 2007), who showed that higher bilirubin levels are positively associated with increased ALP and TBARS.

Elevated levels of glucose in the bloodstream and tissues are a primary cause of heightened oxidative stress as seen in diabetes (Hunt et al., 1990). Albumin, the main protein in circulation, acts as a significant antioxidant in bodily fluids, by providing protection against oxidative damage (Bourdon et al., 1999). Hence an increase in the levels of albumin may be observed. However, prolonged periods of high blood sugar can lead to a decrease in albumin levels, and it might even lose its antioxidant effect and become pro-oxidant. This pattern is mirrored in

bilirubin, which also serves as an antioxidant during oxidative stress. Similar tendencies were observed in the investigations carried out by (Hunt et al., 1990; Bourdon et al., 1999; Vítek, 2012). However the increased levels of ALT in response to high free sugar levels may be due to the fact that ALT is also recognized for its significant function in gluconeogenesis as it transforms alanine into pyruvate to facilitate glucose synthesis Similar studies have also observed that the activity of ALT was upregulated in hyperglycemic conditions (Qian et al. 2015; Mousavi et al. 2016; and Alarifi et al. 2017).

Histopathological examination of the liver and kidneys is crucial for identifying and understanding structural and cellular changes indicative of toxicity caused by NPs (Mangalampalli et al. 2018). The liver, known as the body's "metabolic clearinghouse," plays a pivotal role in metabolite breakdown (Zhang et al. 2011). Microscopic examination of the liver at a dose of 500 mg/kg body weight revealed mild inflammatory cell infiltration around the portal vein, sinusoidal dilation, binucleated hepatocytes, along with portal vein dilation and congestion, compared to the control group, while those exposed to 100 mg/kg bw of MnO_2 NPs showed mild sinusoidal dilation and congestion of portal vein. Similar alterations were observed with other metal oxide NPs (Chen et al. 2009; Lei et al. 2008; Li et al. 2012). The detection of inflammatory cells within hepatic tissue suggests that MnO_2-NPs have the ability to interact with enzymes and proteins present in the hepatic interstitium, thereby disrupting the antioxidant defense mechanisms and triggering the production of reactive oxygen species (ROS), ultimately inducing an inflammatory response (Turpaev, 2002). Additionally, the observed increase in the number of binucleate hepatocytes within the experimental groups indicates hepatocytic regeneration, a common response following toxic insult (Kostka et al. 1999). This increase mirrors previous findings associated with NP exposure (Hougaard et al. 2013; Poulsen et al. 2015). Hu et al. (2013) reported that portal vein congestion and dilation could stem from portal hypertension, whereas Puche et al. (2013) linked sinusoidal dilation to

the activation of perisinusoidal cells possessing contractile properties.

The kidney serves as a pivotal organ for blood filtration, rendering them particularly vulnerable to various forms of toxicity (Zhang et al. 2011). Histological examination of renal tissue in both exposure groups in the present study revealed the presence of inflammatory cell infiltration, alongside distortion of the glomerular structures. Inflammatory macrophages represent the primary population of infiltrating immune cells, in individuals with kidney damage (Tsokos et al. 2024). Conversely, recent clinical and experimental investigations have demonstrated that hyperglycemia prompts inflammation, lipid buildup, and oxidative stress, initiating renal tissue dysfunction by activating multiple signaling pathways (Yang, 2019). And lastly the presence of distorted Glomeruli implies impaired renal filtration (Wahba et al. 2016).

Genotoxicity serves as a crucial parameter in the evaluation of nanoparticle (NP) toxicity. Over numerous years, the comet assay has served as a standard method for evaluating the genotoxicity of potential toxic substances (Dumala et al. 2017). Our findings indicate a slight rise in % tail DNA following MnO_2-NP treatment across the experimental groups. However, this increase did not reach statistical significance when compared to the control group. These findings align with those reported by Singh et al. (2013).

6. SUMMARY

In recent years, extensive research has delved into harnessing threadlike nanoscale MnO_2 particles for diverse applications, benefiting from advancements in nanotechnological domains such as nano-optics, nanoelectronics, pharmacology, chemistry, and metallurgy. This progress has spurred heightened production of dispersed MnO_2 nanoparticles, facilitating their integration into matrices for nanomagnetic materials, sorbents, accelerators, semiconductor thermistors, and other innovative uses. However, despite such promising applications MnO_2-NPs may pose health and safety risks, as well as raise socio-economic and ethical concerns

The follow up study was undertaken to study the acute toxicity of MnO_2-NPs on Mus musculus, where in 15 mice were randomly divided into 3 groups with 1 control group and 2 Exp Groups. The mice were then subjected to oral gavage with 2 different concentrations of MnO_2-NPs (300 mg/kg body weight and 500 mg/kg body weight) for a period of 14 days. The impact of MnO_2-NPs on the genetic material, morphology, liver and kidney function of Mus musculus was assessed. The results indicate that oral administration of MnO_2-NPs did not induce any severe adverse effects on the mice.

An increase in both enzymatic and nonenzymatic antioxidant levels was observed, suggesting the generation of reactive oxygen species (ROS). This likely led to the damage of the hepatocyte membranes, resulting in elevated levels of the liver enzyme ALT and creatinine in the kidneys, along with mild morphological changes in liver and kidney tissues. However, over time, antioxidants were able to neutralize these ROS before they could cause significant toxic effects, such as single-stranded DNA breaks, as evidenced by the absence of genotoxic effects, presence of binucleated hepatocytes in the histopathological examinations of the liver, indicating regeneration and proliferation of hepatocytes, and infiltration of inflammatory cells in the kidneys, suggesting the clearance of these nanoparticles by the immune cells.

6.1 CONCLUSIONS

The results of the present study indicates a relatively low toxicity hazard in the liver and kidneys of mice after acute oral administration of nanoscale MnO_2. The possible mechanisms of this toxicity can be attributed to the free radical production with stimulation of oxidative stress, high sugar levels and inflammatory responses as revealed by changes in antioxidants levels and histopathological examinations.

6.2 FUTURE PROSPECTS

- Chronic toxicity studies on the effect of MnO_2-NPs can be conducted via the oral route in mice.
- The effects of MnO_2-NPs on immunological parameters can be assessed.
- The impact of MnO_2-NPs on the pancreas can also be studied, given their potential role in inducing hyperglycemia and hence the production of ROS thereby suggesting another mechanism for their toxicity.
- Detoxification studies concerning MnO_2-NPs in mice can be undertaken

7. REFERENCES

Afeseh Ngwa, H., Kanthasamy, A., Gu, Y., Fang, N., Anantharam, V., & Kanthasamy, A. G. (2011). Manganese nanoparticle activates mitochondrial dependent apoptotic signaling and autophagy in dopaminergic neuronal cells. Toxicology and Applied Pharmacology, 256(3), 227–240. https://doi.org/10.1016/j.taap.2011.07.018

Affrald R, J., M, N., & Narayan, S. (2022). A comprehensive review of manganese dioxide nanoparticles and strategy to overcome toxicity. Nanomedicine Journal, Online First. https://doi.org/10.22038/nmj.2022.66131.1694

Agency for Toxic Substances and Disease Registry (ATSDR). 2012. Toxicological profile for Manganese. Atlanta, GA: U.S. Department of Health and Human Services, Public Health Service.https://wwwn.cdc.gov/TSP/PHS/PHS.aspx?phsid=100&toxid=23#

Ahamed, M., Akhtar, M. J., Siddiqui, M. A., Ahmad, J., Musarrat, J., Al-Khedhairy, A. A., AlSalhi, M. S., & Alrokayan, S. A. (2011). Oxidative stress mediated apoptosis induced by nickel ferrite nanoparticles in cultured A549 cells. Toxicology, 283(2–3), 101–108. https://doi.org/10.1016/j.tox.2011.02.01

Akçan, R., Aydogan, H. C., Yildirim, M. Ş., TaştekiN, B., & Sağlam, N. (2020). Nanotoxicity: A challenge for future medicine. TURKISH JOURNAL OF MEDICAL SCIENCES, 50(4), 1180–1196. https://doi.org/10.3906/sag-1912-209

Al-Mamary, M., Al-Habori, M., Al-Aghbari, A. M., & Baker, M. M. (2002). Investigation into the toxicological effects of Catha edulis leaves: A short term study in animals. Phytotherapy Research, 16(2), 127–132. https://doi.org/10.1002/ptr.835

Alomari, G., Al-Trad, B., Hamdan, S., Aljabali, A., Al-Zoubi, M., Bataineh, N., Qar, J., & Tambuwala, M. M. (2020). Gold nanoparticles attenuate albuminuria by inhibiting podocyte injury in a rat model of diabetic nephropathy. Drug Delivery and Translational Research, 10(1), 216–

226. https://doi.org/10.1007/s13346-019-00675-6

Annabi Berrahal, A., Nehdi, A., Hajjaji, N., Gharbi, N., & El-Fazâa, S. (2007). Antioxidant enzymes activities and bilirubin level in adult rat treated with lead. Comptes Rendus. Biologies, 330(8), 581–588. https://doi.org/10.1016/j.crvi.2007.05.007

Ashrafi Hafez, A., Naserzadeh, P., Mortazavian, A. M., Mehravi, B., Ashtari, K., Seydi, E., & Salimi, A. (2019). Comparison of the effects of MnO 2 -NPs and MnO 2 -MPs on mitochondrial complexes in different organs. Toxicology Mechanisms and Methods, 29(2), 86–94. https://doi.org/10.1080/15376516.2018.1512693

Augustin, M., Yezerska, O., Fenske, D., Bardenhagen, I., Westphal, A., Knipper, M., Plaggenborg, T., Kolny-Olesiak, J., & Parisi, J. (2015). Mechanistic study on the activity of manganese oxide catalysts for oxygen reduction reaction in an aprotic electrolyte. Electrochimica Acta, 158, 383–389. https://doi.org/10.1016/j.electacta.2015.01.163

Azeh Engwa, G., Udoka Ferdinand, P., Nweke Nwalo, F., & N. Unachukwu, M. (2019). Mechanism and health effects of heavy metal toxicity in humans. In O. Karcioglu & B. Arslan (Eds.), Poisoning in the Modern World—New Tricks for an Old Dog? IntechOpen. https://doi.org/10.5772/intechopen.82511

Baraka-Vidot, J., Guerin-Dubourg, A., Dubois, F., Payet, B., Bourdon, E., & Rondeau, P. (2013). New insights into deleterious impacts of in vivo glycation on albumin antioxidant activities. Biochimica et Biophysica Acta (BBA) - General Subjects, 1830(6), 3532–3541. https://doi.org/10.1016/j.bbagen.2013.01.019

Baral, A., Satish, L., Das, D. P., Sahoo, H., & Ghosh, M. K. (2017). Construing the interactions between MnO 2 nanoparticle and bovine serum albumin: Insight into the structure and stability of a protein–nanoparticle complex. New Journal of Chemistry, 41(16), 8130–8139. https://doi.org/10.1039/C7NJ01227F

Beauchamp, C., & Fridovich, I. (1971). Superoxide dismutase: Improved assays and an assay applicable to acrylamide gels. Analytical Biochemistry, 44(1), 276–287. https://doi.org/10.1016/0003-2697(71)90370-8

Bergna, H. E. (Ed.). (1994). The colloid chemistry of silica (Vol. 234). American Chemical Society. https://doi.org/10.1021/ba-1994-0234

European Commission. Joint Research Centre. (2018). Mapping nanomedicine terminology in the regulatory landscape. Publications Office. https://data.europa.eu/doi/10.2760/753829

Brod, J., & Sirota, J. H. (1948). The renal clearance of endogenous “creatinine” in man. Journal of Clinical Investigation, 27(5), 645–654. https://doi.org/10.1172/JCI102012

Bourdon, E., Loreau, N., & Blache, D. (1999). Glucose and free radicals impair the antioxidant properties of serum albumin. FASEB journal : official publication of the Federation of American Societies for Experimental Biology, 13(2), 233–244. https://doi.org/10.1096/fasebj.13.2.233

Carroll, Nicholas V., et al. “The determination of glycogen in liver and muscle by use of anthrone reagent.” *Journal of Biological Chemistry*, vol. 220, no. 2, June 1956, pp. 583–93. *DOI.org (Crossref)*, https://doi.org/10.1016/S0021-9258(18)65284-6.

Chandel, M., & Jain, G. C. (2016). Manganese chloride induced hepatic and renal toxicity in wistar rats. Toxicology International (Formerly Indian Journal of Toxicology), 23(3), 212. https://doi.org/10.22506/ti/2016/v23/i3/146713

Chen, H., & He, J. (2008). Facile synthesis of monodisperse manganese oxide nanostructures and their application in water treatment. The Journal of Physical Chemistry C, 112(45), 17540–17545. https://doi.org/10.1021/jp806160g

Chen, J., Dong, X., Zhao, J., & Tang, G. (2009). In vivo acute toxicity of titanium dioxide nanoparticles to mice after intraperitioneal injection. Journal of applied toxicology : JAT, 29(4), 330–337. https://doi.org/10.1002/jat.1414

Chen, Q., Xue, Y., & Sun, J. (2013). Kupffer cell-mediated hepatic injury induced by silica nanoparticles in vitro and in vivo. International Journal of Nanomedicine, 8(1), 1129–1140. https://doi.org/10.2147/IJN.S42242

Chinde, S., & Grover, P. (2017). Toxicological assessment of nano and micron-sized tungsten oxide after 28 days repeated oral administration to Wistar rats. Mutation Research/Genetic Toxicology and Environmental Mutagenesis, 819, 1–13. https://doi.org/10.1016/j.mrgentox.2017.05.003

Chtourou, Y., Garoui, E., Boudawara, T., & Zeghal, N. (2013). Therapeutic efficacy of silymarin from milk thistle in reducing manganese-induced hepatic damage and apoptosis in rats. Human & Experimental Toxicology, 32(1), 70–81. https://doi.org/10.1177/0960327112455674

Chtourou, Y., Garoui, E. M., Boudawara, T., & Zeghal, N. (2014). Protective role of silymarin against manganese-induced nephrotoxicity and oxidative stress in rat. Environmental Toxicology, 29(10), 1147–1154. https://doi.org/10.1002/tox.21845

Clarke, C., & Upson, S. (2017). A global portrait of the manganese industry—A socioeconomic perspective. NeuroToxicology, 58, 173–179. https://doi.org/10.1016/j.neuro.2016.03.013

Contera, S., Bernardino De La Serna, J., & Tetley, T. D. (2020). Biotechnology, nanotechnology and medicine. Emerging Topics in Life Sciences, 4(6), 551–554. https://doi.org/10.1042/ETLS20200350

Crossgrove, J., & Zheng, W. (2004). Manganese toxicity upon overexposure. NMR in Biomedicine, 17(8), 544–553. https://doi.org/10.1002/nbm.931

Davies, K. J., Lin, S. W., & Pacifici, R. E. (1987). Protein damage and degradation by oxygen radicals. IV. Degradation of denatured protein. The Journal of biological chemistry, 262(20), 9914–9920.

De Groot, F. (2001). High-resolution x-ray emission and x-ray absorption spectroscopy. Chemical Reviews, 101(6), 1779–1808. https://doi.org/10.1021/cr9900681

De Jesus, R. A., De Assis, G. C., Oliveira, R. J. D., Costa, J. A. S., Da Silva, C. M. P., Iqbal, H. M. N., & Ferreira, L. F. R. (2024). Metal/metal oxide nanoparticles: A revolution in the biosynthesis and medical applications. Nano-Structures & Nano-Objects, 37, 101071. https://doi.org/10.1016/j.nanoso.2023.101071

Delatte, N. J. (2001). Lessons from roman cement and concrete. Journal of Professional Issues in Engineering Education and Practice, 127(3), 109–115. https://doi.org/10.1061/(ASCE)1052-3928(2001)127:3(109)

Dobrakowski, M., Zalejska-Fiolka, J., Wielkoszyński, T., Świętochowska, E., & Kasperczyk, S. (2014). The effect of occupational exposure to lead on the non-enzymatic antioxidant system. Medycyna Pracy, 65(4), 443–451. https://doi.org/10.13075/mp.5893.00025

Dorman, D. C. (2001). Influence of dietary manganese on the pharmacokinetics of inhaled manganese sulfate in male cd rats. Toxicological Sciences, 60(2), 242–251. https://doi.org/10.1093/toxsci/60.2.242

Dreher, K. L. (2003). Health and environmental impact of nanotechnology: Toxicological assessment of manufactured nanoparticles. Toxicological Sciences, 77(1), 3–5. https://doi.org/10.1093/toxsci/kfh041

Drobne, D. (2007). Nanotoxicology for safe and sustainable nanotechnology. Archives of Industrial Hygiene and Toxicology, 58(4), 471–478. https://doi.org/10.2478/v10004-007-0040-4

Dumala, N., Mangalampalli, B., Chinde, S., Kumari, S. I., Mahoob, M., Rahman, M. F., & Grover, P. (2017). Genotoxicity study of nickel oxide nanoparticles in female Wistar rats after acute oral exposure. Mutagenesis, 32(4), 417–427. https://doi.org/10.1093/mutage/gex007

Edwards, P. P., & Thomas, J. M. (2007). Gold in a metallic divided state—From faraday to present-day nanoscience. Angewandte Chemie International Edition, 46(29), 5480–5486. https://doi.org/10.1002/anie.200700428

Elder, A., Gelein, R., Silva, V., Feikert, T., Opanashuk, L., Carter, J., Potter, R., Maynard, A., Ito, Y., Finkelstein, J., & Oberdörster, G. (2006). Translocation of inhaled ultrafine manganese oxide particles to the centralnervous system. Environmental Health Perspectives, 114(8), 1172–1178. https://doi.org/10.1289/ehp.9030

Faraday, M. (1857). The bakerian lecture: Experimental relations of gold (And other metals) to light. Philosophical Transactions of the Royal Society of London Series I, 147, 145–181. https://ui.adsabs.harvard.edu/abs/1857RSPT..147..145F

Feng, L., Xie, R., Wang, C., Gai, S., He, F., Yang, D., Yang, P., & Lin, J. (2018). Magnetic targeting, tumor microenvironment-responsive intelligent nanocatalysts for enhanced tumor ablation. ACS Nano, 12(11), 11000–11012. https://doi.org/10.1021/acsnano.8b05042

Fischer, H. C., & Chan, W. C. (2007). Nanotoxicity: The growing need for in vivo study. Current Opinion in Biotechnology, 18(6), 565–571. https://doi.org/10.1016/j.copbio.2007.11.008

Frick, R., Müller-Edenborn, B., Schlicker, A., Rothen-Rutishauser, B., Raemy, D. O., Günther, D., Hattendorf, B., Stark, W., & Beck-Schimmer, B. (2011). Comparison of manganese oxide nanoparticles and manganese sulfate with regard to oxidative stress, uptake and apoptosis in alveolar epithelial cells. Toxicology Letters, 205(2), 163–172. https://doi.org/10.1016/j.toxlet.2011.05.1037

Friedman, H. “Correction. Modification of Determination of Urea by the Diacetyl Monoxime Method.” *Analytical Chemistry*, vol. 25, no. 6, June 1953, pp. 990–990. *DOI.org (Crossref)*, https://doi.org/10.1021/ac60078a600.

Fu, P. P., Xia, Q., Hwang, H.-M., Ray, P. C., & Yu, H. (2014). Mechanisms of nanotoxicity: Generation of reactive oxygen species. Journal of Food and Drug Analysis, 22(1), 64–75. https://doi.org/10.1016/j.jfda.2014.01.005

Gandhi, D., Rudrashetti, A. P., & Rajasekaran, S. (2022). The impact of environmental and occupational exposures of manganese on pulmonary, hepatic, and renal functions. Journal of Applied Toxicology, 42(1), 103–129. https://doi.org/10.1002/jat.4214

Gao, G., Ze, Y., Li, B., Zhao, X., Zhang, T., Sheng, L., Hu, R., Gui, S., Sang, X., Sun, Q., Cheng, J., Cheng, Z., Wang, L., Tang, M., & Hong, F. (2012). Ovarian dysfunction and gene-expressed characteristics of female mice caused by long-term exposure to titanium dioxide nanoparticles. Journal of Hazardous Materials, 243, 19–27. https://doi.org/10.1016/j.jhazmat.2012.08.049

Ghosh, S. K. (2020). Diversity in the family of manganese oxides at the nanoscale: From fundamentals to applications. ACS Omega, 5(40), 25493–25504. https://doi.org/10.1021/acsomega.0c03455

Godkar, P. B. (1994). Clinical Biochemistry-Principles and Practice. Bhalani Publ, 118(32), 233-238.

Gupta, R., & Xie, H. (2018). Nanoparticles in daily life: Applications, toxicity and regulations. Journal of Environmental Pathology, Toxicology and Oncology, 37(3), 209–230. https://doi.org/10.1615/JEnvironPatholToxicolOncol.2018026009

Hao, L., Xue, L., Huang, F., Cai, G., Qi, W., Zhang, M., Han, Q., Wang, Z., & Lin, J. (2020). A microfluidic biosensor based on magnetic nanoparticle separation, quantum dots labeling and mno2 nanoflower amplification for rapid and sensitive detection of salmonella typhimurium. Micromachines, 11(3), 281. https://doi.org/10.3390/mi11030281

Hemmadi, V. (2016). Estimation of gsh. https://doi.org/10.13140/RG.2.1.5181.6088

Hickman, D. L., Johnson, J., Vemulapalli, T. H., Crisler, J. R., & Shepherd, R. (2017).Commonly used animal models. In Principles of Animal Research (pp. 117–175). Elsevier. https://doi.org/10.1016/B978-0-12-802151-4.00007-4

Hodes, G. (2007). When small is different: Some recent advances in concepts and applications of nanoscale phenomena. Advanced Materials, 19(5), 639–655. https://doi.org/10.1002/adma.200601173

Horváth, E., Máté, Z., Takács, S., Pusztai, P., Sápi, A., Kónya, Z., Nagymajtényi, L., & Papp, A. (2012). General and electrophysiological toxic effects of manganese in rats following subacute administration in dissolved and nanoparticle form. The Scientific World Journal, 2012, 1–7. https://doi.org/10.1100/2012/520632

Hougaard, K. S., Jackson, P., Kyjovska, Z. O., Birkedal, R. K., De Temmerman, P. J., Brunelli, A., Verleysen, E., Madsen, A. M., Saber, A. T., Pojana, G., Mast, J., Marcomini, A., Jensen, K. A., Wallin, H., Szarek, J., Mortensen, A., & Vogel, U. (2013). Effects of lung exposure to carbon nanotubes on female fertility and pregnancy. A study in mice. Reproductive toxicology (Elmsford, N.Y.), 41, 86–97. https://doi.org/10.1016/j.reprotox.2013.05.006

Hsu, B. Y. W., Kirby, G., Tan, A., Seifalian, A. M., Li, X., & Wang, J. (2016). Relaxivity and toxicological properties of manganese oxide nanoparticles for MRI applications. RSC Advances, 6(51), 45462–45474. https://doi.org/10.1039/C6RA04421B

Hu, L. S., George, J., & Wang, J. H. (2013). Current concepts on the role of nitric oxide in portal hypertension. World journal of gastroenterology, 19(11), 1707–1717. https://doi.org/10.3748/wjg.v19.i11.1707

Hussain, S. M., Javorina, A. K., Schrand, A. M., Duhart, H. M., Ali, S. F., & Schlager, J. J. (2006). The interaction of manganese nanoparticles with pc-12 cells induces dopamine depletion. Toxicological Sciences, 92(2), 456–463. https://doi.org/10.1093/toxsci/kfl020

Iavicoli, I., Fontana, L., & Nordberg, G. (2016). The effects of nanoparticles on the renal system. Critical Reviews in Toxicology, 46(6), 490–560. https://doi.org/10.1080/10408444.2016.1181047

Ismail, H.T.H. Hematobiochemical Disturbances and Oxidative Stress After Subacute Manganese Chloride Exposure and Potential Protective Effects of Ebselen in Rats. Biol Trace Elem Res 187, 452–463 (2019). https://doi.org/10.1007/s12011-018-1395-x

Jafarzadeh Samanai, R., Heydarnejad, M.s., & Aghayeevanda, S.. (2016). The Effects Of Silver Nanoparticles On Creatinine, Bun And Blood Electrolytes In Laboratory Male Mice (mus Musculus). Journal Of Shahrekord University Of Medical Sciences, 17(5), 64-73. Sid. Https://sid.ir/paper/58927/en

Khan, M. I., Mohammad, A., Patil, G., Naqvi, S. A. H., Chauhan, L. K. S., & Ahmad, I. (2012). Induction of ROS, mitochondrial damage and autophagy in lung epithelial cancer cells by iron oxide nanoparticles. Biomaterials, 33(5), 1477–1488. https://doi.org/10.1016/j.biomaterials.2011.10.080

Kim, J. H., Kim, J. H., Kim, K.-W., Kim, M. H., & Yu, Y. S. (2009). Intravenously administered gold nanoparticles pass through the blood–retinal barrier depending on the particle size, and induce no retinal toxicity. Nanotechnology, 20(50), 505101. https://doi.org/10.1088/0957-4484/20/50/505101

Kim, K. B., & Lee, B. M. (1997). Oxidative stress to DNA, protein, and antioxidant enzymes (Superoxide dismutase and catalase) in rats treated with benzo(A)pyrene. Cancer Letters, 113(1–2), 205–212. https://doi.org/10.1016/S0304-3835(97)04610-7

King, E. J., & Armstrong, A. R. (1934). A convenient method for determining serum and bile phosphatase activity. Canadian Medical Association Journal, 31(4), 376–381.

Komura, J., & Sakamoto, M. (1992). Effects of manganese forms on biogenic amines in the brain and behavioral alterations in the mouse: Long-term oral administration of several manganese compounds. Environmental Research, 57(1), 34–44. https://doi.org/10.1016/S0013-9351(05)80017-9

Kostka, G., Palut, D., Kopeć-Szlezak, J., & Ludwicki, J. K. (2000). Early hepatic changes in rats induced by permethrin in comparison with DDT. Toxicology, 142(2), 135–143. https://doi.org/10.1016/s0300-483x(99)00164-x

Kumari, M., Rajak, S., Singh, S. P., Kumari, S. I., Kumar, P. U., Murty, U. S. N., Mahboob, M., Grover, P., & Rahman, M. F. (2012). Repeated oral dose toxicity of iron oxide nanoparticles: Biochemical and histopathological alterations in different tissues of rats. Journal of Nanoscience and Nanotechnology, 12(3), 2149–2159. https://doi.org/10.1166/jnn.2012.5796

Lee, P.-C., Li, N.-S., Hsu, Y.-P., Peng, C., & Yang, H.-W. (2019). Direct glucose detection in whole blood by colorimetric assay based on glucose oxidase-conjugated graphene oxide/MnO 2 nanozymes. The Analyst, 144(9), 3038–3044. https://doi.org/10.1039/C8AN02440E

Lei, N., Wang, M., Zhang, L., Xiao, S., Fei, C., Wang, X., Zhang, K., Zheng, W., Wang, C., Yang, R., & Xue, F. (2015). Effects of low molecular weight yeast β-glucan on antioxidant and immunological activities in mice. International Journal of Molecular Sciences, 16(9), 21575–21590. https://doi.org/10.3390/ijms160921575

Lei, R., Wu, C., Yang, B., Ma, H., Shi, C., Wang, Q., Wang, Q., Yuan, Y., & Liao, M. (2008). Integrated metabolomic analysis of the nano-sized copper particle-induced hepatotoxicity and nephrotoxicity in rats: a rapid in vivo screening method for nanotoxicity. Toxicology and applied pharmacology, 232(2), 292–301. https://doi.org/10.1016/j.taap.2008.06.026

Li, N., Georas, S., Alexis, N., Fritz, P., Xia, T., Williams, M. A., Horner, E., & Nel, A. (2016). A work group report on ultrafine particles (American academy of allergy, asthma & immunology): Why ambient ultrafine and engineered nanoparticles should receive special attention for possible adverse health outcomes in human subjects. Journal of Allergy and Clinical Immunology, 138(2), 386–396. https://doi.org/10.1016/j.jaci.2016.02.023

Li, X., Kong, X., Zhang, Z., Nan, K., Li, L., Wang, X., & Chen, H. (2012). Cytotoxicity and biocompatibility evaluation of N,O-carboxymethyl chitosan/oxidized alginate hydrogel for drug delivery application. International journal of biological macromolecules, 50(5), 1299–1305. https://doi.org/10.1016/j.ijbiomac.2012.03.008

Liang, G., Pu, Y., Yin, L., Liu, R., Ye, B., Su, Y., & Li, Y. (2009). Influence of different sizes of titanium dioxide nanoparticles on hepatic and renal functions in rats with correlation to oxidative stress. Journal of Toxicology and Environmental Health, Part A, 72(11–12), 740–745. https://doi.org/10.1080/15287390902841516

Limbach, L. K., Wick, P., Manser, P., Grass, R. N., Bruinink, A., & Stark, W. J. (2007). Exposure of engineered nanoparticles to human lung epithelial cells: Influence of chemical composition and catalytic activity on oxidative stress. Environmental Science & Technology, 41(11), 4158–4163. https://doi.org/10.1021/es062629t

Lison, D., Lardot, C., Huaux, F., Zanetti, G., & Fubini, B. (1997). Influence of particle surface area on the toxicity of insoluble manganese dioxide dusts. Archives of Toxicology, 71(12), 725–729. https://doi.org/10.1007/s002040050453

Liu, J., Duan, X., Wang, M., & Su, X. (2019). A label-free fluorescent sensor based on silicon quantum dots–MnO 2 nanosheets for the detection of α-glucosidase and its inhibitor. The Analyst, 144(24), 7398–7405. https://doi.org/10.1039/C9AN01680E

Liu, J., Meng, L., Fei, Z., Dyson, P. J., Jing, X., & Liu, X. (2017). MnO 2 nanosheets as an artificial enzyme to mimic oxidase for rapid and sensitive detection of glutathione. Biosensors and Bioelectronics, 90, 69–74. https://doi.org/10.1016/j.bios.2016.11.046

Liu, Z., Yi, Y., Zhang, S., Zhu, T., Zhu, J., & Wang, J. (2013). Selective catalytic reduction of NOx with NH3 over Mn-Ce mixed oxide catalyst at low temperatures. Catalysis Today, 216, 76–81. https://doi.org/10.1016/j.cattod.2013.06.009

Lobo, V., Patil, A., Phatak, A., & Chandra, N. (2010). Free radicals, antioxidants and functional foods: Impact on human health. Pharmacognosy Reviews, 4(8), 118. https://doi.org/10.4103/0973-7847.70902

Lowry, OliverH., Rosebrough, NiraJ., Farr, A. L., & Randall, RoseJ. (1951). Protein measurement with the folin phenol reagent. Journal of Biological Chemistry, 193(1), 265–275. https://doi.org/10.1016/S0021-9258(19)52451-6

Madejczyk, M. S., Boyer, J. L., & Ballatori, N. (2009). Hepatic uptake and biliary excretion of manganese in the little skate, Leucoraja erinacea. Comparative Biochemistry and Physiology Part C: Toxicology & Pharmacology, 149(4), 566–571. https://doi.org/10.1016/j.cbpc.2008.12.009

Masciangioli, T., & Zhang, W.-X. (2003). Peer reviewed: Environmental technologies at the nanoscale. Environmental Science & Technology, 37(5), 102A-108A. https://doi.org/10.1021/es0323998

Mahmoudi, M., Hofmann, H., Rothen-Rutishauser, B., & Petri-Fink, A. (2012). Assessing the in vitro and in vivo toxicity of superparamagnetic iron oxide nanoparticles. Chemical Reviews, 112(4), 2323–2338. https://doi.org/10.1021/cr2002596

Malik, S., Muhammad, K., & Waheed, Y. (2023). Nanotechnology: A revolution in modern industry. Molecules, 28(2), 661. https://doi.org/10.3390/molecules28020661

Malloy, H. T., & Evelyn, K. A. (1937). The determination of bilirubin with the photoelectric colorimeter. Journal of Biological Chemistry, 119(2), 481–490. https://doi.org/10.1016/S0021-9258(18)74392-5

Mangalampalli, B., Dumala, N., Perumalla Venkata, R., & Grover, P. (2018). Genotoxicity, biochemical, and biodistribution studies of magnesium oxide nano and microparticles in albino wistar rats after 28-day repeated oral exposure. Environmental Toxicology, 33(4), 396–410. https://doi.org/10.1002/tox.22526

Manke, A., Wang, L., & Rojanasakul, Y. (2013). Mechanisms of nanoparticle-induced oxidative stress and toxicity. BioMed Research International, 2013, 1–15. https://doi.org/10.1155/2013/942916

McConnell, R., Islam, T., Shankardass, K., Jerrett, M., Lurmann, F., Gilliland, F., Gauderman, J., Avol, E., Künzli, N., Yao, L., Peters, J., & Berhane, K. (2010). Childhood incident asthma and traffic-related air pollution at home and school. Environmental Health Perspectives, 118(7), 1021–1026. https://doi.org/10.1289/ehp.0901232

Mireles, L. C., Lum, M. A., & Dennery, P. A. (1999). Antioxidant and cytotoxic effects of bilirubin on neonatal erythrocytes. Pediatric research, 45(3), 355–362. https://doi.org/10.1203/00006450-199903000-00011

Mukherjee, S., & Patra, C. R. (2016). Therapeutic application of anti-angiogenic nanomaterials in cancers. Nanoscale, 8(25), 12444–12470. https://doi.org/10.1039/C5NR07887C

Naik, S. R., Javeer, D. S., Gawde, C. S., Palni, S. S., Koli, S. C., Jalmi, S. S., Ghotge, Y. V., Naik, N. U., Fernandes, R., & Velho-Pereira, S. (2021). Larvicidal activity of pristine α-MnO2 nanostructures: An environmentally benign approach for combating mosquito (Diptera: culicidae) menace. Materials Today Communications, 27, 102184. https://doi.org/10.1016/j.mtcomm.2021.102184

Nelson, Norton. “A photometric adaptation of the somogyi method for the determination of glucose.” *Journal of Biological Chemistry*, vol. 153, no. 2, May 1944, pp. 375–80. *DOI.org (Crossref)*, https://doi.org/10.1016/S0021-9258(18)71980-7.

Niehaus, W. G., & Samuelsson, B. (1968). Formation of malonaldehyde from phospholipid arachidonate during microsomal lipid peroxidation. European Journal of Biochemistry, 6(1), 126–130. https://doi.org/10.1111/j.1432-1033.1968.tb00428.x

Niknahad, A. M., Ommati, M. M., Farshad, O., Moezi, L., & Heidari, R. (2020). Manganese-induced nephrotoxicity is mediated through oxidative stress and mitochondrial impairment. Journal of Renal and Hepatic Disorders, 4(2), 1–10. https://doi.org/10.15586/jrenhep.2020.66

N.V. Zaitseva, M.A. Zemlyanova, V.N. Zvezdin, & T.I. Akafieva. (2013). Biological effects of manganese oxide nanoparticles after peroral intake. Journal of Pharmacy and Nutrition Sciences, 3(4), 231–237. https://doi.org/10.6000/1927-5951.2013.03.04.3

Oladipo, O. O., Ayo, J. Olusegun., Ambali, S. F., & Mohammed, B. (2016). Evaluation of hepatorenal impairments in Wistar rats coexposed to low-dose lead, cadmium and manganese: Insights into oxidative stress mechanism. *Toxicology Mechanisms and Methods*, *26*(9), 674–684. https://doi.org/10.1080/15376516.2016.1223242

Oloyede, H., Atiq, Z., Adigun, R., & Salawu, M. (2017). Protective effects of a locally-manufactured device on electromagnetic radiation-induced cellular alterations in rats exposed to mobile phone radiation. Journal of Investigational Biochemistry, 6(1), 11. https://doi.org/10.5455/jib.20170215105236

Park, E.-J., Bae, E., Yi, J., Kim, Y., Choi, K., Lee, S. H., Yoon, J., Lee, B. C., & Park, K. (2010). Repeated-dose toxicity and inflammatory responses in mice by oral administration of silver nanoparticles. Environmental Toxicology and Pharmacology, 30(2), 162–168. https://doi.org/10.1016/j.etap.2010.05.004

Puche, J. E., Saiman, Y., & Friedman, S. L. (2013). Hepatic stellate cells and liver fibrosis. Comprehensive Physiology, 3(4), 1473–1492. https://doi.org/10.1002/cphy.c120035

Qian, K., Zhong, S., Xie, K., Yu, D., Yang, R., & Gong, D. (2015). Hepatic ALT isoenzymes are elevated in gluconeogenic conditions including diabetes and suppressed by insulin at the protein level. Diabetes/Metabolism Research and Reviews, 31(6), 562–571. https://doi.org/10.1002/dmrr.2655

Rashidi, L., & Khosravi-Darani, K. (2011). The applications of nanotechnology in food industry. Critical Reviews in Food Science and Nutrition, 51(8), 723–730. https://doi.org/10.1080/10408391003785417

Reitman, S., & Frankel, S. (1957). A colorimetric method for the determination of serum glutamic oxalacetic and glutamic pyruvic transaminases. American Journal of Clinical Pathology, 28(1), 56–63. https://doi.org/10.1093/ajcp/28.1.56

Roco, M. C. (2011). The long view of nanotechnology development: The National Nanotechnology Initiative at 10 years. Journal of Nanoparticle Research, 13(2), 427–445. https://doi.org/10.1007/s11051-010-0192-z

Sánchez-González, C., López-Chaves, C., Gómez-Aracena, J., Galindo, P., Aranda, P., & Llopis,

Schrand, A. M., Rahman, M. F., Hussain, S. M., Schlager, J. J., Smith, D. A., & Syed, A. F. (2010). Metal-based nanoparticles and their toxicity assessment. WIREs Nanomedicine and Nanobiotechnology, 2(5), 544–568. https://doi.org/10.1002/wnan.103

Sharma, P., Jha, A. B., Dubey, R. S., & Pessarakli, M. (2012). Reactive oxygen species, oxidative damage, and antioxidative defense mechanism in plants under stressful conditions. Journal of Botany, 2012, 1–26. https://doi.org/10.1155/2012/217037

Singh, N. A. (2017). Nanotechnology innovations, industrial applications and patents. Environmental Chemistry Letters, 15(2), 185–191. https://doi.org/10.1007/s10311-017-0612-8

Singh, N. P., McCoy, M. T., Tice, R. R., & Schneider, E. L. (1988). A simple technique for quantitation of low levels of DNA damage in individual cells. Experimental Cell Research, 175(1), 184–191. https://doi.org/10.1016/0014-4827(88)90265-0

Singh, S. P., Kumari, M., Kumari, S. I., Rahman, M. F., Kamal, S. S. K., Mahboob, M., & Grover, P. (2013). Genotoxicity of nano- and micron-sized manganese oxide in rats after acute oral treatment. Mutation Research/Genetic Toxicology and Environmental Mutagenesis, 754(1–2), 39–50. https://doi.org/10.1016/j.mrgentox.2013.04.003

Sinha, A. K. (1972). Colorimetric assay of catalase. *Analytical Biochemistry*, *47*(2), 389–394. https://doi.org/10.1016/0003-2697(72)90132-7

Sulaiman, A. F., Akanji, M. A., Oloyede, O. B., Sulaiman, A. A., Olatunde, A., Joel, E. B., Adewale, T. H., Adeboye, H. A., Idris, S. O., Quadri, A. L., Oyegoke, R. A., & Adeyemi, O. S. (2015). Oral exposure to silver/gold nanoparticles: Status of ratlipid profile, serum metabolites and tissue morphology. *Journal of Medical Science*, *15*(2), 71–79.http://eprints.lmu.edu.ng/2221/

Stallings, W. C., Metzger, A. L., Paitridge, K. A., Fee, J. A., & Ludwig, M. L. (1991). Structure-function relationships in iron and manganese superoxide dismutases. Free Radical Research Communications, 12(1), 259–268. https://doi.org/10.3109/10715769109145794

Sun, P.-P., Lai, C.-S., Hung, C.-J., Dhaiveegan, P., Tsai, M.-L., Chiu, C.-L., & Fang, J.-M. (2021). Subchronic oral toxicity evaluation of gold nanoparticles in male and female mice. *Heliyon*, *7*(3), e06577. https://doi.org/10.1016/j.heliyon.2021.e06577

Rochman, N. T. (2020). Synthesis of manganese ferrite from manganese ore prepared by mechanical milling and its application as an inorganic heat-resistant pigment. Journal of Materials Research and Technology, 9(4), 8497–8506. https://doi.org/10.1016/j.jmrt.2020.05.122

Varela, A. T., Duarte, F. V., Rolo, A. P., Hussain, S., & Palmeira, C. M. (2016). Low-dose, subchronic exposure to silver nanoparticles causes mitochondrial alterations in Sprague–Dawley rats. Nanomedicine, 11(11), 1359–1375. https://doi.org/10.2217/nnm-2016-0049

Tootoonchi, M. H., Hashempour, M., Blackwelder, P. L., & Fraker, C. A. (2017). Manganese oxide particles as cytoprotective, oxygen generating agents. Acta Biomaterialia, 59, 327–337. https://doi.org/10.1016/j.actbio.2017.07.006

Tseng, M. T., Lu, X., Duan, X., Hardas, S. S., Sultana, R., Wu, P., Unrine, J. M., Graham, U., Butterfield, D. A., Grulke, E. A., & Yokel, R. A. (2012). Alteration of hepatic structure and oxidative stress induced by intravenous nanoceria. Toxicology and Applied Pharmacology, 260(2), 173–182. https://doi.org/10.1016/j.taap.2012.02.008

Tulinska, J., Masanova, V., Liskova, A., Mikusova, M. L., Rollerova, E., Krivosikova, Z., Stefikova, K., Uhnakova, I., Ursinyova, M., Babickova, J., Babelova, A., Busova, M., Tothova, L., Wsolova, L., Dusinska, M., Sojka, M., Horvathova, M., Alacova, R., Vecera, Z., … Docekal, B. (2020). Six-week inhalation of CdO nanoparticles in mice: The effects on immune response oxidative stress, antioxidative defense, fibrotic response, and bones. Food and Chemical Toxicology, 136, 110954. https://doi.org/10.1016/j.fct.2019.110954

Vladimirovna Zaitseva, N., & Alexandrovna Zemlyanova, M. (2020). Toxicologic characteristics of nanodisperse manganese oxide: Physical-chemical properties, biological accumulation, and morphological-functional properties at various exposure types. In J. Kanayochukwu Nduka & M. Nageeb Rashed (Eds.), Heavy Metal Toxicity in Public Health. IntechOpen. https://doi.org/10.5772/intechopen.83499

Wahba, N. S., Shaban, S. F., Kattaia, A. A., & Kandeel, S. A. (2016). Efficacy of zinc oxide nanoparticles in attenuating pancreatic damage in a rat model of streptozotocin-induced diabetes. Ultrastructural pathology, 40(6), 358–373. https://doi.org/10.1080/01913123.2016.1246499

Wang, P., Liang, C., Zhu, J., Yang, N., Jiao, A., Wang, W., Song, X., & Dong, X. (2019). Manganese-based nanoplatform as metal ion-enhanced ros generator for combined chemodynamic/photodynamic therapy. ACS Applied Materials & Interfaces, 11(44), 41140–41147. https://doi.org/10.1021/acsami.9b16617

Xu, W., Sun, J., Li, L., Peng, X., Zhang, R., & Wang, B. (2017). Melanin-manganese nanoparticles with ultrahigh efficient clearance in vivo for tumor-targeting T1 magnetic resonance imaging contrast agent. Biomaterials Science, 6(1), 207–215. https://doi.org/10.1039/C7BM00635G

Yang, S. T., Wang, X., Jia, G., Gu, Y., Wang, T., Nie, H., Ge, C., Wang, H., & Liu, Y. (2008). Long-term accumulation and low toxicity of single-walled carbon nanotubes in intravenously exposed mice. Toxicology letters, 181(3), 182–189. https://doi.org/10.1016/j.toxlet.2008.07.020

Yang, X. (2019). Design and optimization of crocetin loaded PLGA nanoparticles against diabetic nephropathy via suppression of inflammatory biomarkers: A formulation approach to preclinical study. Drug Delivery, 26(1), 849–859. https://doi.org/10.1080/10717544.2019.1642417

Yildirim, N. C., Tanyol, M., Yildirim, N., Serdar, O., & Tatar, S. (2018). Biochemical responses of Gammarus pulex to malachite green solutions decolorized by Coriolus versicolor as a biosorbent under batch adsorption conditions optimized with response surface methodology. Ecotoxicology and Environmental Safety, 156, 41–47. https://doi.org/10.1016/j.ecoenv.2018.02.059

Yousefalizadegan, N., Mousavi, Z., Rastegar, T., Razavi, Y., & Najafizadeh, P. (2019). Reproductive toxicity of manganese dioxide in forms of micro- and nanoparticles in male rats. International Journal of Reproductive Biomedicine, 17(5), 361–370. https://doi.org/10.18502/ijrm.v17i5.4603

Zaitseva, N. V., Zemlyanova, M. A., Zvezdin, V. N., Akafieva, T. I., Mazunina, D. L., & Dovbysh, A. A. (2014). The effects of subchronic exposure to manganese oxide nanoparticles on the central nervous system, pero lipid oxidation, and antioxidant enzymes in rats. Health Risk Analysis, (4), 53-62. https://doi.org/10.21668/health.risk/2014.4.09.eng

Zhang, Z., & Kleinstreuer, C. (2011). Computational analysis of airflow and nanoparticle deposition in a combined nasal–oral–tracheobronchial airway model. Journal of Aerosol Science, 42(3), 174–194. https://doi.org/10.1016/j.jaerosci.2011.01.001

Zheng, Y., Zhang, H., Hu, Y., Bai, L., & Xue, J. (2018). MnO nanoparticles with potential application in magnetic resonance imaging and drug delivery for myocardial infarction. International journal of nanomedicine, 13, 6177–6188. https://doi.org/10.2147/IJN.S176404

Zhou, B., Zhao, J., Qiao, Y., Wei, Q., He, J., Li, W., Zhong, D., Ma, F., Li, Y., & Zhou, M. (2018). Simultaneous multimodal imaging and photothermal therapy via renal-clearable manganese-doped copper sulfide nanodots. Applied Materials Today, 13, 285–297. https://doi.org/10.1016/j.apmt.2018.09.011

Zvezdin, V. N., Zemlyanova, M. A., & Akafieva, T. I. (2015). [Inhalation toxicity of nanodispersed manganese oxide aerosol]. Meditsina truda i promyshlennaia ekologiia, 12, 13–16.